

Discovery of Acyl-sulfonamide Na_v1.7 Inhibitors GDC-0276 and GDC-0310

Brian S. Safina, Steven J. McKerrall,* Shaoyi Sun, Chien-An Chen, Sultan Chowdhury, Qi Jia, Jun Li, Alla Y. Zenova, Jean-Christophe Andrez, Girish Bankar, Philippe Bergeron, Jae H. Chang, Elaine Chang, Jun Chen, Richard Dean, Shannon M. Decker, Antonio DiPasquale, Thilo Focken, Ivan Hemeon, Kuldip Khakh, Amy Kim, Rainbow Kwan, Andrea Lindgren, Sophia Lin, Jonathan Maher, Janette Mezeyova, Dinah Misner, Karen Nelkenbrecher, Jodie Pang, Rebecca Reese, Shannon D. Shields, Luis Sojo, Tao Sheng, Henry Verschoof, Matthew Waldbrook, Michael S. Wilson, Zhiwei Xie, Clint Young, Tanja S. Zabka, David H. Hackos, Daniel F. Ortwine, Andrew D. White, J.P. Johnson, Jr., C. Lee Robinette, Christoph M. Dehnhardt, Charles J. Cohen, and Daniel P. Sutherlin*



Cite This: *J. Med. Chem.* 2021, 64, 2953–2966



Read Online

ACCESS |



Metrics & More

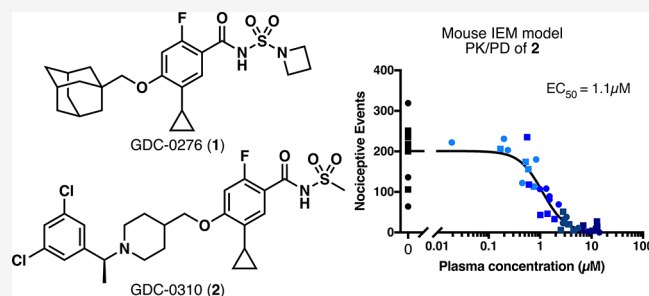


Article Recommendations



Supporting Information

ABSTRACT: Na_v1.7 is an extensively investigated target for pain with a strong genetic link in humans, yet in spite of this effort, it remains challenging to identify efficacious, selective, and safe inhibitors. Here, we disclose the discovery and preclinical profile of GDC-0276 (1) and GDC-0310 (2), selective Na_v1.7 inhibitors that have completed Phase 1 trials. Our initial search focused on close-in analogues to early compound 3. This resulted in the discovery of GDC-0276 (1), which possessed improved metabolic stability and an acceptable overall pharmacokinetics profile. To further derisk the predicted human pharmacokinetics and enable QD dosing, additional optimization of the scaffold was conducted, resulting in the discovery of a novel series of N-benzyl piperidine Na_v1.7 inhibitors. Improvement of the metabolic stability by blocking the labile benzylic position led to the discovery of GDC-0310 (2), which possesses improved Na_v selectivity and pharmacokinetic profile over 1.



INTRODUCTION

Chronic pain is a highly prevalent unmet medical need, with the CDC estimating that in the United States (US) alone, 50.0 million people experience chronic pain—pain on most days or every day for the past 6 months—and 19.6 million people experience chronic pain that limits their life or work activities.¹ The voltage-gated sodium channel Na_v1.7 is an essential mediator of painful stimuli.² In particular, Na_v1.7 has been linked to pain sensation in humans through the identification of loss-of-function mutations in SCN9A, the gene that encodes Na_v1.7, which causes profound insensitivity to pain.^{3,4} These results have been further recapitulated and extensively studied through genetic experiments in both germ-line and adult-inducible knockout mice.^{5,6} Together, these data provide strong validation that inhibition of Na_v1.7 could produce substantial pain relief and support the use of preclinical rodent models for evaluation of pharmacodynamic and analgesic effects.

The wealth of information linking Na_v1.7 to pain has motivated substantial efforts to discover potent and subtype-selective Na_v1.7 inhibitors.^{7,8} Recently, significant efforts have

focused on acylsulfonamide and arylsulfonamide inhibitor scaffolds that bind to voltage-sensing domain IV (VSD4) and stabilize an inactivated state of the channel.^{9–13} In particular, this effort has been motivated by the recognition that compounds in these series are capable of exhibiting selectivity over other members of the voltage gated sodium channel family. This is a critical challenge in the discovery of safe Na_v1.7 inhibitors as other Na_v isoforms are responsible for an array of essential functions in, among many other tissues, the CNS (Na_v1.1, Na_v1.2, Na_v1.6), skeletal muscle (Na_v1.4), and heart (Na_v1.5).^{14,15} Despite progress, balancing potency, selectivity, in vivo activity, and DMPK properties remains challenging in these series of compounds.⁸

Received: January 11, 2021

Published: March 8, 2021



We have previously disclosed our efforts to optimize a series of acylsulfonamide $\text{Na}_v1.7$ inhibitors resulting in the discovery of **3** and **4** (Figure 1).¹⁶ These compounds contain a common

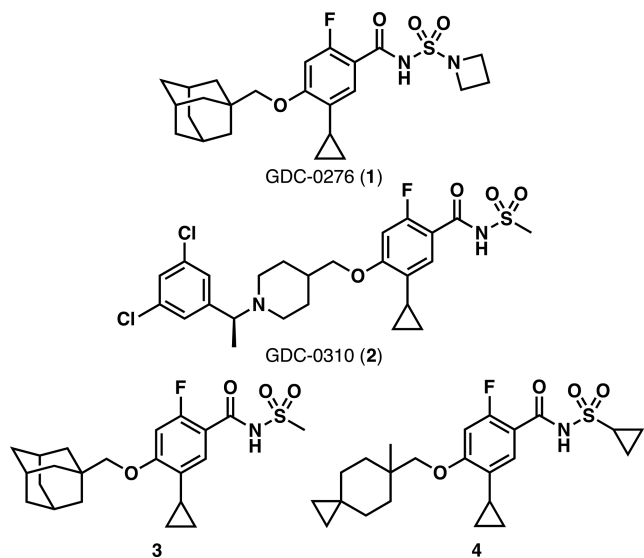


Figure 1. GDC-0276 (**1**), GDC-0310 (**2**), and previously described acylsulfonamide $\text{Na}_v1.7$ inhibitors.

anionic sulfonamide moiety that makes critical interactions with a conserved arginine residue in the binding site.¹⁶ Key to the identification of these compounds was the recognition that saturated groups, such as the adamantane or cyclohexane in **3**

and **4**, respectively, conferred excellent $\text{Na}_v1.7$ potency and provided reasonable selectivity over $\text{Na}_v1.5$, which we viewed as the most critical off-target isoform due to the relationship between $\text{Na}_v1.5$ function and human cardiotoxicity.¹⁵ However, these saturated groups also led to significant metabolic liabilities for these compounds that resulted in poor predicted pharmacokinetics in humans. Here, we describe our efforts to improve on the pharmacokinetic (PK) properties of **3**, resulting in **1** (GDC-0276) and **2** (GDC-0310), two development candidates which have progressed to Phase 1 studies.

RESULTS AND DISCUSSION

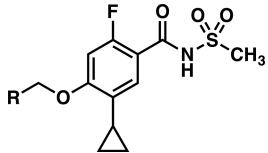
Our optimization campaign began with sulfonamide **3** (Table 1). Compound **3** showed excellent $\text{Na}_v1.7$ potency in both radioligand binding and sodium influx assays and moderate selectivity against $\text{Na}_v1.5$ as measured in a sodium influx assay. This assay format tended to underpredict the selectivity seen in electrophysiology (EP) assays; however, it was useful for rank ordering compounds and identifying significant changes in selectivity. Due to the extremely high plasma protein binding of this series of inhibitors, compounds were also assayed in the influx assay in the presence of 3 mg/mL of bovine serum albumin (Flux PS). Compounds showing shifts >2-fold in this assay tended to perform poorly in our in vivo PK/PD model despite high levels of potency and were thus avoided. The major liability of **3** was its high clearance in vitro, with scaled hepatic clearances in human liver microsomes and hepatocytes nearly at the rate of human liver blood flow (20.7 mL/min/kg). To improve the predicted half-life and allow for

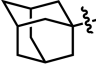
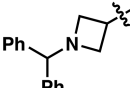
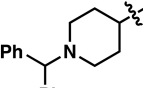
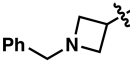
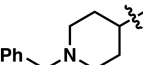
Table 1. Structure Activity Relationships Leading to GDC-0276 (**1**)

Ex	R	$\text{Na}_v1.7$ K_i (nM) ^a	$\text{Na}_v1.7$ Flux (nM) ^b	$\text{Na}_v1.5$ Flux (nM) / Fold ^b	$\text{Na}_v1.7$ Flux PS (fold) ^c	HLM / HH (mL/min/kg) ^d	LogD _{7.4} / LLE ^e
3		1.6	25	1100 / 44x	1.2x	19 / 17	3.3 / 5.5
5		1.1	14	260 / 19x	1x	18 / 16	3.2 / 5.7
6		4.0	38	750 / 20x	2.9x	16 / 6.7	3.4 / 5.0
7		2.3	110	110 / 1x	0.7x	11 / 12	3.8 / 4.8
8		2.2	160	1500 / 9x	0.4x	8.5 / <6.2	4.4 / 4.2
1		1.1	49	870 / 18x	1x	10 / 11	3.1 / 5.8

^a $h\text{Na}_v1.7$ K_i from a radioligand binding assay. ^b IC_{50} of sodium influx in cells transfected with $h\text{Nav}1.7$ or $h\text{Nav}1.5$. ^c IC_{50} of sodium influx in the presence of 3 mg/mL BSA. ^dScaled hepatic clearance from human liver microsomes and hepatocytes. ^eLLE was calculated using $\text{Na}_v1.7$ K_i and LogD_{7.4} (LLE = $pK_i - \text{LogD}_{7.4}$).

Table 2. Discovery of the N-Benzyl Piperidine Scaffold



Ex	R	Na _v 1.7 K _i (nM) ^a	Na _v 1.7 Flux (nM) ^b	Na _v 1.5 Flux (nM) / Fold ^b	Na _v 1.7 Flux PS (fold) ^c	HLM / HH (mL/min/kg) ^d	LogD _{7.4} / LLE ^e
3		1.6	25	1100 / 44x	1.2x	19 / 17	3.3 / 5.5
9		5.5	23	1100 / 48x	8.3x	6.7 / 15	1.8 / 6.4
10		3.6	66	590 / 8.9x	0.6x	5.5 / <6.2	2.7 / 5.7
11		1800	25000	>30000 / >1.2x	1.0x	ND / ND	0.1 / 5.6
12		140	3200	>30000 / >9.1x	1.4x	4.8 / 15	0.3 / 6.7

^a*h*Na_v1.7 K_i from a radioligand binding assay. ^bIC₅₀ of sodium influx in cells transfected with *h*Nav1.7 or *h*Nav1.5. ^cIC₅₀ of sodium influx in the presence of 3 mg/mL BSA. ^dScaled hepatic clearance from human liver microsomes and hepatocytes. ^eLLE was calculated using Na_v1.7 K_i and LogD_{7.4} (LLE = pK_i - LogD_{7.4}).

reasonable dosing, achieving a decrease in clearance was essential.

While metabolite identification experiments consistently indicated the adamantane group was a major site of metabolism, substitution of the adamantane with polar or blocking groups, including fluorine, universally reduced potency to unacceptable levels.¹⁶ Additionally, while the adamantane group could be replaced with other saturated groups, as in **4**, the overall profile still did not result in acceptable predicted human pharmacokinetics.¹⁶ We hypothesized that compounds of this class could be metabolized by P450 isoforms that recognize anionic substrates such as 2C8, 2C9, and 2C19 and that modifying the anionic sulfonamide could result in improved stability (see [Supporting Information](#)).¹⁷ Subsequent CYP reaction phenotyping on **1** confirmed that it was primarily metabolized by CYP2C8 and provided validation of our hypothesis. To this end, we prepared a number of analogues modifying the methylsulfonamide, a selection of which are shown in [Table 1](#). Cyclopropane **5** was representative of the general profile of nonpolar alkyl sulfonamides, which had good potency and Na_v1.5 selectivity but showed no improvement in metabolic stability. More polar sulfonamides such as oxetane **6** tended to slightly reduce the potency and provide improvements in metabolic stability which were too inconsistent to be leveraged.

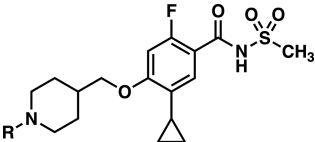
Modifying the acylsulfonamide to an acylsulfamoyl group proved more fruitful. In particular, sulfamoyl groups substituted with a cyclic amine provided the best balance of potency and metabolic stability. While morpholine **7** had

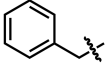
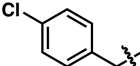
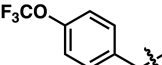
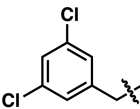
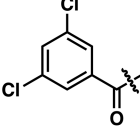
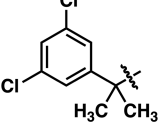
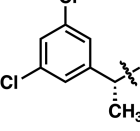
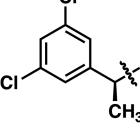
acceptable Na_v1.7 potency and an improvement in HLM and HH stability, poor Na_v1.5 selectivity was a concern, as at least 10-fold was desired in this assay. Pyrrolidine **8** also showed an increase in metabolic stability but with only modest Na_v1.5 selectivity and a poor LLE. Azetidine **1** had increased potency, acceptable Na_v1.5 selectivity, improved HLM and HH stability, and the highest LLE of all sulfamoyl-containing compounds surveyed. After additional characterization (*vide infra*), **1** was predicted to have acceptable human pharmacokinetics and was selected as our first development candidate, GDC-0276.

While we believed **1** had improved predicted pharmacokinetics over **3**, high plasma protein binding and low predicted volume of distribution led to significant uncertainty in the predicted half-life. Additionally, **1** was predicted to require BID dosing to achieve sufficient target coverage, and QD dosing was viewed as a significant advantage. Therefore, we continued our optimization campaign to find compounds with further improved metabolic stability to improve the PK profile and derisk uncertainty in the predicted PK of **1**. Furthermore, there was room for improvement in the selectivity profile of **1**, in particular over Na_v1.5, which we viewed as the key peripheral off-target.

Subsequent optimization efforts focused on replacing the adamantane group with polar saturated groups that might provide a significant change in the overall metabolism. Further exploration of replacements for the adamantane led to the discovery that suitably substituted azetidine and piperidine rings could provide a tractable scaffold ([Table 2](#)). Benzhydryl substituted azetidine **9** and piperidine **10** showed reasonable

Table 3. Discovery of GDC-0310 (2)



Ex	R	Na _v 1.7 K _i (nM) ^a	Na _v 1.7 Flux (nM) ^b	Na _v 1.5 Flux (nM) / Fold ^b	Na _v 1.7 Flux PS (fold) ^c	HLM / HH (mL/min/kg) ^d	LogD _{7.4} / LLE ^e
12		140	3200	>30000 / >9x	1.4x	4.8 / 15	0.3 / 6.5
13		22	42	27000 / 667x	1.7x	9.9 / 15	ND / ND
14		7.7	31	17000 / 531x	11x	9.9 / ND	1.2 / 6.9
15		2.4	120	7000 / 58x	1.3x	9.7 / 15	2.0 / 6.6
16		9.8	34	6400 / 183x	7.1x	8.6 / 7.5	0.9 / 7.1
17		0.8	26	3900 / 144x	1.3x	7.8 / < 6.2	3.9 / 5.1
18		1.8	34	1800 / 53x	3.7x	17 / 16	2.2 / 6.5
2		1.8	16	1500 / 94x	1.1x	9.6 / < 6.2	2.3 / 6.4

^a*h*Na_v1.7 K_i from a radioligand binding assay. ^bIC₅₀ of sodium influx in cells transfected with *h*Nav1.7 or *h*Nav1.5. ^cIC₅₀ of sodium influx in the presence of 3 mg/mL BSA. ^dScaled hepatic clearance from human liver microsomes and hepatocytes. ^eLLE was calculated using Na_v1.7 K_i and LogD_{7.4} (LLE = pK_i - LogD_{7.4}).

potency and selectivity over Na_v1.5 and an overall reduction in lipophilicity relative to 3. Additionally, piperidine 10 showed a promising increase in metabolic stability in both human liver microsomes and hepatocytes. Paring back the large and lipophilic benzhydryl group to a benzyl group in azetidines 11 or piperidines 12 resulted in a significant reduction in potency. However, this potency reduction was accompanied by a substantial reduction in LogD_{7.4}, which resulted in 11 and 12 having an LLE comparable to 3. In spite of its low lipophilicity, 12 showed mixed results in metabolic stability assays, with high clearance observed in human hepatocytes. Taken together, these results led us to continue our investigation of N-benzyl substituted piperidines with the aim of improving the potency and metabolic stability of this novel scaffold.

Further optimization focused on improving potency through incorporation of lipophilic substituents on the benzyl group (Table 3). Simple substitutions such as para-chloro 13 and para-trifluoromethoxy 14 led to improved potency, a maintenance of high LLE, and acceptable Na_v1.5 selectivity. After extensive exploration of phenyl substituents, we arrived at meta-dichloro 15 as possessing the best balance of potency, selectivity, and LLE. While this compound represented a promising lead, it continued to suffer from poor hepatocyte stability. In contrast to our experience with 1, replacing the methanesulfonamide with sulfamoyl groups did not meaningfully improve the metabolic stability in the scaffold. In vitro metabolism studies on this series of compounds indicated that they were consistently metabolized via N-dealkylation, leading

to the unsubstituted piperidine. Therefore, we sought to improve the metabolic stability through substitution of the metabolically labile benzylic position.

Gratifyingly, we found that piperidine amide **16** provided a significant improvement in the hepatocyte stability over **15**. While this validated our hypothesis, **16** showed decreased potency and a high shift in the presence of plasma protein (vide supra). After additional SAR investigations, gem-dimethyl compound **17** was found to possess an excellent balance of potency, Na_v1.5 selectivity, and hepatocyte stability. While the overall profile of **17** looked promising, we were concerned about the high lipophilicity and low LLE. To determine if we could maintain the potency/selectivity profile while reducing the lipophilicity, we prepared the monomethyl analogues **18** and **2**. Both **18** and **2** showed good potency, Na_v1.5 selectivity, and lipophilicity; however, they surprisingly differed dramatically in their hepatocyte stability. While the *R* enantiomer **18** had a scaled hepatic clearance of 16 mL/min/kg in hepatocytes, comparable to parent **15**, the *S* enantiomer **2** showed clearance of <6.2 mL/min/kg. This is a particularly stark example of the impact of chirality on P450 mediated metabolism.¹⁸ Based on the overall profile described below, **2** was progressed as our second development candidate, GDC-0310.

The Na_v selectivities of **1** and **2** were characterized by voltage-clamp studies using the PatchExpress platform (Table 4). Due to the compound's preferential binding to the

Table 4. Na_v Selectivity of **1** and **2**^a

	<i>h</i> Na _v 1.7 IC ₅₀	<i>h</i> Na _v 1.1 IC ₅₀ (fold)	<i>h</i> Na _v 1.2 IC ₅₀ (fold)	<i>h</i> Na _v 1.4 IC ₅₀ (fold)	<i>h</i> Na _v 1.5 IC ₅₀ (fold)	<i>h</i> Na _v 1.6 IC ₅₀ (fold)
1	0.4 nM	10.6 nM (26×)	18.9 nM (47×)	8.5 nM (21×)	51 nM (127×)	480 nM (1200×)
2	0.6 nM	202 nM (337×)	38 nM (63×)	3.4 nM (6×)	551 nM (918×)	198 nM (330×)

^aNav1.X potency measured by voltage clamp on the PatchExpress platform.

inactivated state of the channel, inhibition of each isoform was measured while maintaining a holding potential at depolarizing voltages that promote steady-state inactivation of the channel.¹³ Slow equilibration of potent compounds requires a protocol that maintains channels in the high affinity state (inactivated) for a prolonged period of time to facilitate equilibration of block. This approach allowed for accurate determination of the potency and molecular selectivities of **1** and **2** across Na_vs. Compound **1** showed a high level of selectivity over Na_v1.6, >100-fold selectivity over Na_v1.5, and moderate selectivity over Na_v1.1, Na_v1.2, and Na_v1.4. In contrast, **2** had significantly improved selectivity over a number of isoforms, with >300-fold selectivity over Na_v1.1, Na_v1.5, and Na_v1.6. The selectivity over Na_v1.2 was 63-fold, while the selectivity over Na_v1.4 was a relatively low 6-fold. In spite of the low selectivity versus Na_v1.4, no obvious in vivo effects due to blocking Na_v1.4 were observed. This is potentially due to both the marked state-dependence of this series of Na_v1.7 inhibitors such that inhibition is much weaker at voltages in which inactivation is removed and the fact that muscle fibers that express Na_v1.4 maintain a significantly more negative resting membrane potential relative to the sensory neurons that express Na_v1.7. Overall, the selectivity data supported

further evaluation of **1** and **2** as selective Na_v1.7 inhibitors and reinforced the improved profile of **2** over **1**.

The DMPK profiles of **1** and **2** are shown in Table 5. In addition to the improvement in human hepatocyte stability

Table 5. DMPK Properties of **1** and **2**^a

(a)	HH Cl _{Hep} (mL/min/kg) ^a	MDCK P _{app} (10 ⁶ cm/s) ^b	<i>h</i> F _u (%) ^c	kinetic solubility (μM) ^d	CYP3A4 IC ₅₀ (μM)
1	11	4.7	0.025	5.3	>10
2	<6.2	11	0.196	52	>10

(b)	1			2		
	rat	dog	cyno	rat	dog	cyno
Hep Cl _{Hep} (mL/min/kg) ^a	23	<7.8	18	11	<7.8	13
<i>F</i> _u (%) ^b	0.013	0.005	0.025	0.278	0.157	0.129
Cl _p (mL/min/kg) ^c	5.1	0.40	2.3	1.4	0.091	0.87
<i>V</i> _{ss} (L/kg) ^e	0.38	0.17	0.30	0.60	0.33	0.29
<i>T</i> _{1/2} (hr) ^e	0.95	5.5	1.6	5.0	46	4.4
<i>F</i> % ^e	34	50	30	68	~100	82

^a(a) In vitro human pharmacokinetic profile of **1** and **2**. (b) In vitro and in vivo pharmacokinetic profile in Sprague–Dawley rats, Beagle dogs, and cynomolgus monkeys. ^bScaled hepatic clearance from hepatocytes. ^cPassive A–B permeability in a WT-MDCKI transwell assay. ^dUnbound fraction reported as a percentage (e.g., 0.025% = 0.00025). ^eKinetic solubility of a DMSO solution in pH 7.4 PBS. ^fIn vivo pharmacokinetic parameters determined from 1 mg/kg (rat, cyno) or 0.5 mg/kg (dog) IV dose. ^gDetermined using 5 mg/kg (rat), 1.0 mg/kg (dog), or 2.0 mg/kg (cyno) oral dose in a suspension of 0.5% methylcellulose, 0.2% Tween 80 in water.

described above, **2** also showed improved permeability in MDCK cells and increased kinetic solubility. The improvement in permeability was surprising in light of the strongly zwitterionic nature of **2**, which has an acidic p*K*_a of 3.9 and a basic p*K*_a of 8.6. The improvement in metabolic stability was also reflected in the improved in vivo PK of **2** compared to **1**. Compound **1** showed low clearance across all species, however, the high plasma protein binding resulted in a low volume of distribution and a short to moderate half-life of 0.95–5.5 h across species. Additionally, **1** had low to moderate oral bioavailability, likely due to its relatively poor solubility. Both of these effects were observed in the human PK of **1**, which exhibited a less than dose proportional exposure and evidence of delayed absorption using a powder in capsule formulation.¹⁹ When dosed with a cyclodextrin solution formulation, **1** showed a half-life of 3.8–5.3 h, consistent with the range of half-lives observed in preclinical species. This further validated the need for a backup compound. In contrast, **2** showed extremely low clearance in vivo, resulting in a half-life of 4.4–46 h in preclinical species in spite of the low volume of distribution. The high permeability and improved solubility of **2** also resulted in moderate to high oral bioavailability across species. Overall, **2** provided a superior in vitro and in vivo pharmacokinetic profile over **1**.

To confirm the activity of **1** and **2** in vivo we tested both compounds in a previously described inherited erythromelalgia (IEM) mouse model (Figure 2).²⁰ Briefly, this model tests the ability of compounds to block a response to aconitine, a plant alkaloid that causes abnormal opening of sodium channels, in a transgenic mouse containing a human Na_v1.7 gain-of-function variant. Aconitine causes a specific effect in these transgenic

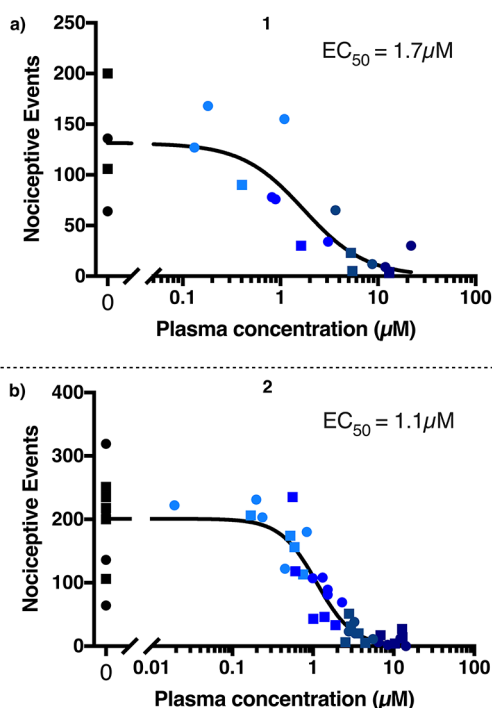


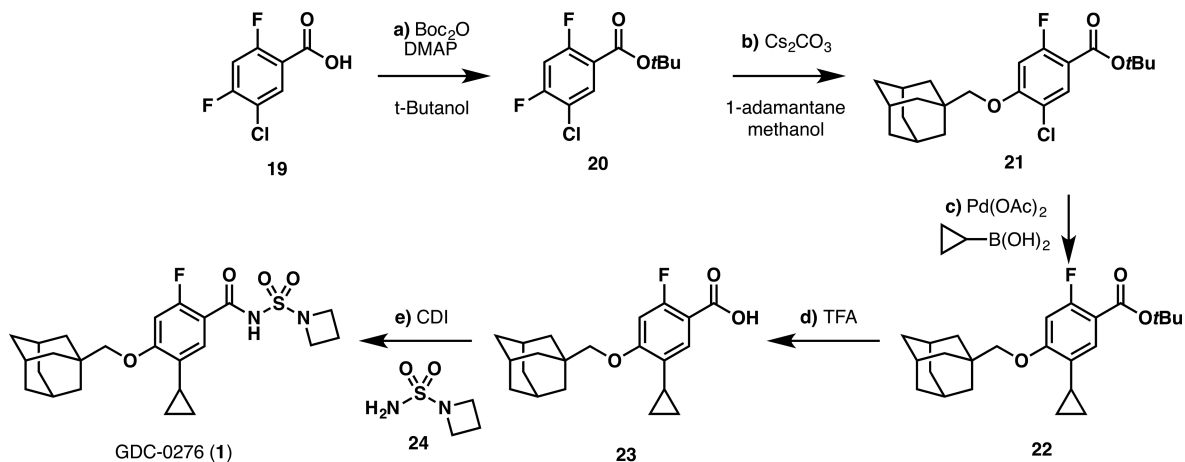
Figure 2. IEM aconitine assay PK/PD of **1** and **2**. (a) PK/PD of **1** in the IEM model. (b) PK/PD of **2** in the IEM model. Each dot represents an individual animal measurement.

mice while having no impact on wild type mice, and the resulting PK/PD relationship is dependent on human $\text{Na}_v1.7$ potency. $\text{Na}_v1.7$ inhibitors show comparable activity in this model to traditional inflammatory and neuropathic pain models.²⁰ In this model, **1** and **2** both showed a concentration dependent reduction in nociceptive events, with a EC_{50} s of 1.7 μM and 1.1 μM , respectively. Correcting for mouse PPB indicated an $\text{EC}_{50,u}$ of 0.42 nM for **1** and an $\text{EC}_{50,u}$ of 3.5 nM for **2**. Both values are comparable to the IC_{50} for inhibition of $h\text{Na}_v1.7$ reported above. Notably, both **1** and **2** compared very favorably with the previously disclosed development candidate PF-05089771, which had an $\text{EC}_{50} > 18 \mu\text{M}$ in this assay.^{9,20}

Chemistry. The synthesis of GDC-0276 (**1**) and its analogues began with benzoic acid **19** (Scheme 1).¹⁶ *tert*-butyl ester formation with Boc_2O and DMAP provided *tert*-butyl ester **20**. Next, the adamantane group was incorporated through an $\text{S}_{\text{N}}\text{Ar}$ reaction with 1-adamantane methanol, giving **21** as a single regioisomer. Introduction of the aryl cyclopropane was affected via an alkyl-Suzuki reaction with cyclopropylboronic acid catalyzed by $\text{Pd}(\text{OAc})_2$ and PCy_3 to give **22**. Next, deprotection of the *tert*-butyl ester was facilitated by treatment with TFA to give penultimate benzoic acid **23**. Finally, formation of the acylsulfamoyl group was completed by activation of the carboxylic acid with CDI and reaction with sulfonamide **24** to form GDC-0276 (**1**). The overall sequence was highly efficient, producing GDC-0276 in 5 linear steps from commercial starting materials. The route was also highly scalable and could be further improved to support 100 kg synthesis.²¹ Compounds **5–8** were prepared using an analogous sequence by substituting in the requisite sulfonamide.

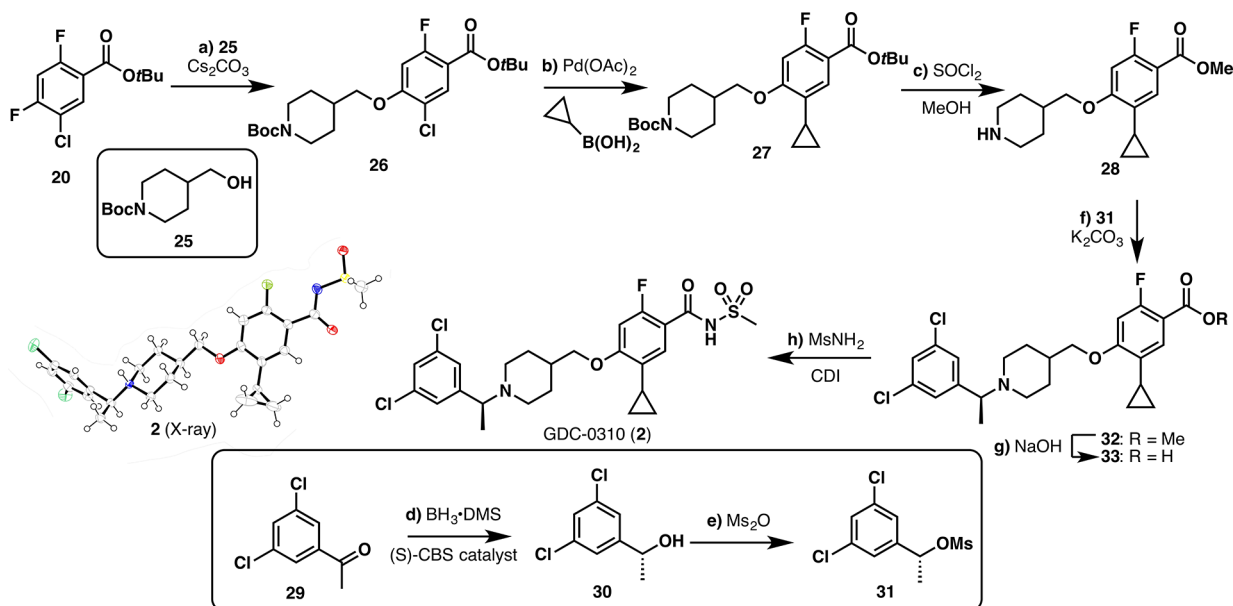
The synthesis of GDC-0310 (**2**) began with *tert*-butyl ester **20** (Scheme 2). Nucleophilic aromatic substitution with alcohol **25** provided Boc-piperidine intermediate **26** as a single regioisomer. Introduction of the aryl cyclopropane was again achieved via an alkyl-Suzuki reaction with cyclopropylboronic acid catalyzed by $\text{Pd}(\text{OAc})_2$ and PCy_3 to give **27**. Treatment with SOCl_2 in MeOH affected deprotection of both the piperidine Boc and *tert*-butyl ester followed by subsequent methyl ester formation to provide the unprotected piperidine **28**. Synthesis of the chiral electrophile **31** began with acetophenone **29**. Reduction of the carbonyl with $\text{BH}_3\cdot\text{DMS}$ and (*S*)-CBS catalyst produced alcohol **30** in 98.3% ee. Subsequent mesylation with Ms_2O produced mesylate **31**. Combining amine **28** and mesylate **31** in the presence of Cs_2CO_3 effected smooth $\text{S}_{\text{N}}2$ substitution to give *N*-benzyl piperidine **32** with the requisite (*S*)-stereochemistry. Hydrolysis of the methyl ester with NaOH provided benzoic acid **33**, which could be activated with CDI and reacted with methansulfonamide to produce GDC-0310 (**2**). The absolute configuration of **2** was unambiguously confirmed through a small molecule X-ray crystal structure. The overall synthesis provided **2** in 7 linear steps from commercially available

Scheme 1. Synthesis of GDC-0276 (**1**)^a



^aReagents and conditions: (a) Boc_2O , DMAP, *t*-BuOH, 60 °C, 18 h, 90%. (b) Cs_2CO_3 , 1-adamantane methanol, DMSO, 80 °C, 4 h, 52%. (c) $\text{Pd}(\text{OAc})_2$, cyclopropyl boronic acid, $\text{PCy}_3\cdot\text{HBF}_4$, K_3PO_4 , PhMe, H_2O , 100 °C, 18 h, 86%. (d) TFA, CH_2Cl_2 , rt, 2 h, 71%. (e) CDI, azetidine-1-sulfonamide, DBU, THF, rt, 16 h, 91%.

Scheme 2. Synthesis of GDC-0310 (2)



^aReagents and conditions: (a) Cs_2CO_3 , **25**, DMSO, rt, 1 h, 60%. (b) $\text{Pd}(\text{OAc})_2$, PCy_3 · HBF_4 , cyclopropylboronic acid, K_3PO_4 , PhMe, H_2O , 100 °C, 16 h, 74%. (c) SOCl_2 , MeOH, reflux, 16 h, 70%. (d) (S)-CBS catalyst, BH_3 ·DMS, THF, rt, 4 h, 79%, 98.3% ee. (e) Ms_2O , Et_3N , CH_2Cl_2 , 0 °C to rt, 2 h, 94%. (f) **31**, K_2CO_3 , 4-methyl-2-pentanone, H_2O , 85 °C, 16 h, 99%. (g) NaOH, THF, H_2O , 70 °C, 16 h, 97%. (h) CDI, MsNH_2 , K_2CO_3 , EtOAc, 70 °C, 4 h, 79%. Absolute stereochemistry of **2** was unambiguously confirmed by single-crystal X-ray diffraction.

starting materials. Again, the synthesis was highly scalable and an improved early development synthesis allowed the preparation of 6.5 kg of **2**.²² Analogues **9–18** were prepared in an analogous fashion as described in the [Experimental Section](#).

CONCLUSION

Acylsulfonamide Na_v 1.7 inhibitors **3** and **4** showed promising biological activity and selectivity but suffered from inadequate ADME properties. Initial optimization focused on the hypothesis that modifying the anionic sulfonamide could improve the metabolic stability, and resulted in the discovery of acylsulfamoyl groups which exhibited superior profiles in liver microsomes and hepatocytes. This ultimately led to the discovery of GDC-0276 (**1**) which possessed improved metabolic stability sufficient for selection as a development candidate.¹⁹ To further derisk the pharmacokinetic properties of **1** and to allow for QD dosing, we conducted a search for a novel scaffold, ultimately replacing the lipophilic adamantane group with more polar saturated amines. The resulting N-benzyl piperidine scaffold still suffered from poor in vitro metabolic stability, which could be improved by substituting the metabolically labile benzylic position, resulting in GDC-0310 (**2**). GDC-0310 (**2**) showed substantially improved Na_v selectivity and ADME properties, which supported its selection as our second development candidate. GDC-0276 (**1**) and GDC-0310 (**2**) have both completed Phase 1 studies, but their subsequent development has been discontinued.¹⁹ Full results of our clinical and nonclinical experience with **1** and **2** will be reported in due course.

EXPERIMENTAL SECTION

General Methods. Unless otherwise specified, commercially available reagents and solvents were used without further purification. Yields refer to chromatographically and spectroscopically (¹H NMR)

homogeneous materials unless otherwise stated. NMR experiments were performed with Bruker Avance III 300, 400, or 500 MHz spectrometers. ¹H, ¹⁹F, and ¹³C NMR data are reported as chemical shifts (δ) in parts per million (ppm) and are calibrated using residual undeuterated solvent as an internal reference. Proton spectra are reported as chemical shift, multiplicity (s = singlet, d = doublet, t = triplet, q = quartet, m = multiplet, and br = broad), coupling constant in Hz, and number of protons. Carbon and fluorine NMR spectra are reported as chemical shift alone. High resolution mass spectrometry was performed on a Dionex Ultimate 3000 coupled with Thermo Scientific Q Exactive HRMS using ESI as ionization source. The LC separation was done on a Phenomenex XB-C18, 1.7 mm, 50 × 2.1 mm column at a flow rate of 0.4 mL/min. MPA (mobile phase A) was water with 0.1% FA and MPB (mobile phase B) was acetonitrile with 0.1% FA. The gradient started at 2% MPB and ended at 98% MPB over 7 min and held at 98% MPB for 1.5 min following an equilibration for 1.5 min. LC column temperature was 40 °C. UV absorbance was collected by a DAD detector and mass spec full scan was applied to all experiments. Optical rotation was measured on an Autopol VI Automatic Polarimeter from Rudolph Research Analytical. Reactions were monitored by walkup Shimadzu HPLC/UV system with LC-10AD solvent pump, FVC-10AL, DGU-14A degasser, SPD-M10A UV detector, CTO-10AC column oven, using the elution gradient 10–80% (2.5 ML/4LTF in acetonitrile) over 4 min and holding at 80% for 2 min at a flow rate of 1.2 mL/min. Routine purification was performed using Teledyne Isco Combiflash Rf utilizing Silicycle HP columns. Reverse-phase purifications were carried out using a Gilson GX-281 system with a 322 solvent pump, 159 UV-vis detector and a Xtimate C18 150 × 25 mm × 5 μm column using MeCN/ H_2O gradients described below. Preparative SFC separations were carried out as described below. Analytical purity of all final compounds was greater than 95% as determined by LCMS using 254 nM UV detection unless otherwise stated.

4-((Adamantan-1-yl)methoxy)-N-(azetidin-1-ylsulfonyl)-5-cyclopropyl-2-fluorobenzamide (1, GDC-0276). A mixture of **23** (12.4 g, 36.1 mmol) in anhydrous tetrahydrofuran (250 mL) was treated with carbonyldiimidazole (7.3 g, 45.1 mmol). The resulting mixture was refluxed under nitrogen for 1 h. The reaction mixture was cooled to room temperature and then treated with azetidine-1-

sulfonamide (6.4 g, 46.9 mmol) and 1,8-diazabicycloundec-7-ene (13.5 mL, 90.3 mmol). The resulting solution was stirred for 16 h at ambient temperature under nitrogen. The reaction solution was quenched with anhydrous methanol (12 mL) and stirred for 2 h. The mixture was diluted with ethyl acetate, washed with a 1:1 mixture of 3 M hydrochloric acid:brine, a 1:1 mixture of 1 M hydrochloric acid:brine, and brine. The organic layer was dried over anhydrous Na₂SO₄, filtered and concentrated in vacuo. The solid was crystallized with methanol to yield the title compound (15.13 g, 91%). ¹H NMR (400 MHz, DMSO-*d*₆) δ 11.57 (s, 1H), 7.15 (d, *J* = 8.2 Hz, 1H), 6.93 (d, *J* = 12.9 Hz, 1H), 4.04 (t, *J* = 7.7 Hz, 4H), 3.65 (s, 2H), 2.22–2.11 (m, 2H), 2.09–1.96 (m, 4H), 1.78–1.63 (m, 12H), 0.95–0.87 (m, 2H), 0.71–0.65 (m, 2H). ¹³C NMR (101 MHz, DMSO) δ 162.32 (d, *J* = 238.8 Hz), 162.21 (d, *J* = 10.7 Hz), 158.62, 127.96, 127.00, 100.42 (d, *J* = 26.4 Hz), 78.79, 51.97 (2C), 39.31 (3C), 37.04 (3C), 34.00, 27.97 (3C), 15.10, 9.64, 7.56 (2C). ¹⁹F NMR (376 MHz, DMSO-*d*₆) δ –112.31. HRMS (ESI-FTMS) *m/z* [M + H]⁺ Calcd for C₂₄H₃₂O₄N₂FS 463.2061; Found 463.2061.

(S)-5-Cyclopropyl-4-((1-(3,5-dichlorophenyl)ethyl)piperidin-4-yl)methoxy)-2-fluoro-N-(methylsulfonyl)benzamide (2, GDC-0310). To a solution of 33 (40 g, 85.7 mmol) in EtOAc (400 mL) was added CDI (21.6 g, 120 mmol). The mixture was heated to 35 °C and stirred for 2 h. Methanesulfonamide (12.6 g, 128 mmol) and K₂CO₃ (23.7 g, 171 mmol) were added, and the mixture was heated to 70 °C and stirred for 4 h. Water was added, and the mixture was extracted with EtOAc. The organic fractions were concentrated and suspended in EtOAc. The suspension was heated to 70 °C and cooled to 10 °C over 10 h. The resulting solids were collected by filtration to yield 2 (37.0 g, 79% yield) as a white solid. ¹H NMR (400 MHz, DMSO-*d*₆) δ 7.41 (t, *J* = 1.9 Hz, 1H), 7.36 (d, *J* = 1.9 Hz, 2H), 7.18 (d, *J* = 8.3 Hz, 1H), 6.84 (d, *J* = 13.0 Hz, 1H), 3.94 (d, *J* = 5.9 Hz, 2H), 3.66 (q, *J* = 6.8 Hz, 1H), 3.23 (s, 3H), 2.99–2.93 (m, 1H), 2.83 (d, *J* = 11.6 Hz, 1H), 2.16–2.05 (m, 2H), 2.00 (tt, *J* = 8.4, 5.3 Hz, 1H), 1.86–1.72 (m, 3H), 1.48–1.33 (m, 2H), 1.32 (d, *J* = 6.8 Hz, 3H), 0.92–0.83 (m, 2H), 0.68–0.60 (m, 2H). Exchangeable NH not observed. ¹³C NMR (101 MHz, DMSO-*d*₆) δ 164.57, 160.90 (d, *J* = 18.1 Hz), 159.59 (d, *J* = 259.6 Hz), 147.98, 133.92 (2C), 127.20, 126.94, 126.41 (2C), 126.15, 114.55 (d, *J* = 9.4 Hz), 100.25 (d, *J* = 26.4 Hz), 72.99, 62.57, 49.89, 48.76, 41.30, 35.37, 28.56 (2C), 17.71, 9.14, 6.88 (2C). ¹⁹F NMR (376 MHz, DMSO-*d*₆) δ –112.66. HRMS (ESI-FTMS) *m/z* [M + H]⁺ Calcd for C₂₅H₃₀O₄N₂Cl₂FS 543.1282; Found 543.1281. [α]_D +0.008 (c 2.0, CHCl₃).

4-((Adamantan-1-yl)methoxy)-5-cyclopropyl-N-(cyclopropylsulfonyl)-2-fluorobenzamide (5). Compound 5 was synthesized using the general procedure for the synthesis of 1, substituting azetidine-1-sulfonamide for cyclopropylanesulfonamide. ¹H NMR (400 MHz, DMSO-*d*₆) δ 11.78 (s, 1H), 7.14 (d, *J* = 8.2 Hz, 1H), 6.93 (d, *J* = 13.1 Hz, 1H), 3.65 (s, 2H), 3.07 (tt, *J* = 7.7, 5.1 Hz, 1H), 2.10–1.96 (m, 4H), 1.78–1.63 (m, 12H), 1.19–1.04 (m, 4H), 0.96–0.84 (m, 2H), 0.74–0.62 (m, 2H). HRMS (ESI-FTMS) *m/z* [M + H]⁺ Calcd for C₂₄H₃₁O₄NFS 448.1952; Found 448.1953.

4-((Adamantan-1-yl)methoxy)-5-cyclopropyl-2-fluoro-N-(oxetan-3-ylsulfonyl)benzamide (6). Compound 6 was synthesized using the general procedure for the synthesis of 1, substituting azetidine-1-sulfonamide for oxetane-3-sulfonamide. ¹H NMR (400 MHz, DMSO-*d*₆) δ 7.33 (d, *J* = 8.4 Hz, 1H), 6.97 (d, *J* = 13.6 Hz, 1H), 5.34 (t, *J* = 5.7 Hz, 1H), 4.96 (dd, *J* = 12.7, 3.6 Hz, 1H), 4.80 (ddd, *J* = 13.1, 9.3, 7.1 Hz, 2H), 3.98–3.77 (m, 1H), 3.65 (d, *J* = 18.7 Hz, 2H), 2.02 (ddt, *J* = 14.0, 5.8, 2.9 Hz, 4H), 1.73 (d, *J* = 12.2 Hz, 3H), 1.69–1.63 (m, 9H), 0.98–0.90 (m, 1H), 0.94–0.83 (m, 1H), 0.68–0.55 (m, 2H). Exchangeable NH not observed. HRMS (ESI-FTMS) *m/z* [M + H]⁺ Calcd for C₂₄H₃₁O₅NFS 464.1901; Found 464.1902.

4-((Adamantan-1-yl)methoxy)-5-cyclopropyl-2-fluoro-N-(morpholinosulfonyl)benzamide (7). Compound 7 was synthesized using the general procedure for the synthesis of 1, substituting azetidine-1-sulfonamide for morpholine-4-sulfonamide. ¹H NMR (400 MHz, DMSO-*d*₆) δ 11.69 (s, 1H), 7.12 (d, *J* = 8.2 Hz, 1H), 6.91 (d, *J* = 12.9 Hz, 1H), 3.68–3.60 (m, 6H), 3.45–3.34 (m, 1H),

3.26 (ddd, *J* = 5.4, 3.0, 1.3 Hz, 3H), 2.02 (dt, *J* = 17.4, 3.4 Hz, 4H), 1.78–1.63 (m, 12H), 0.96–0.83 (m, 2H), 0.74–0.62 (m, 2H). HRMS (ESI-FTMS) *m/z* [M + H]⁺ Calcd for C₂₅H₃₄O₅N₂FS 493.2167; Found 493.2169.

4-((Adamantan-1-yl)methoxy)-5-cyclopropyl-2-fluoro-N-(pyrrolidin-1-ylsulfonyl)benzamide (8). Compound 8 was synthesized using the general procedure for the synthesis of 1, substituting azetidine-1-sulfonamide for pyrrolidine-1-sulfonamide. ¹H NMR (400 MHz, DMSO-*d*₆) δ 11.51 (s, 1H), 7.10 (d, *J* = 8.1 Hz, 1H), 6.90 (d, *J* = 12.9 Hz, 1H), 3.64 (s, 2H), 3.44–3.35 (m, 4H), 2.09–1.96 (m, 4H), 1.88–1.77 (m, 4H), 1.77–1.63 (m, 12H), 0.95–0.83 (m, 2H), 0.74–0.59 (m, 2H). HRMS (ESI-FTMS) *m/z* [M + H]⁺ Calcd for C₂₅H₃₄O₄N₂FS 477.2218; Found 477.2217.

4-((1-Benzhydrylazetid-3-yl)methoxy)-5-cyclopropyl-2-fluoro-N-(methylsulfonyl)benzamide (9). Compound 9 was prepared from S2 and methanesulfonamide following the general procedure for the synthesis of 2. See Supporting Information for the synthesis of S2. ¹H NMR (400 MHz, DMSO-*d*₆) δ 11.83 (s, 1H), 7.45–7.39 (m, 4H), 7.28 (t, *J* = 7.6 Hz, 4H), 7.22–7.13 (m, 3H), 6.94 (d, *J* = 12.8 Hz, 1H), 4.50 (s, 1H), 4.21 (d, *J* = 6.2 Hz, 2H), 3.27 (s, 2H), 3.24 (s, 3H), 3.03 (s, 2H), 2.89 (d, *J* = 14.5 Hz, 1H), 2.05 (tt, *J* = 8.4, 5.3 Hz, 1H), 0.94–0.85 (m, 2H), 0.70–0.61 (m, 2H). HRMS (ESI-FTMS) *m/z* [M + H]⁺ Calcd for C₂₈H₃₀O₄N₂FS 509.1905; Found 509.1906.

4-((1-Benzhydrylpiperidin-4-yl)methoxy)-5-cyclopropyl-2-fluoro-N-(methylsulfonyl)benzamide (10). Compound 10 was prepared using the general procedure for the synthesis of 2, substituting 31 for benzhydryl chloride in the reaction preparing 32. ¹H NMR (400 MHz, DMSO-*d*₆) δ 11.88 (s, 1H), 7.77–7.58 (m, 5H), 7.56–7.33 (m, 5H), 7.13 (d, *J* = 8.3 Hz, 1H), 6.99 (d, *J* = 13.0 Hz, 1H), 5.55 (d, *J* = 9.1 Hz, 1H), 3.99 (d, *J* = 5.9 Hz, 2H), 3.28 (s, 3H), 3.15–2.97 (m, 2H), 2.15–1.95 (m, 4H), 1.95–1.79 (m, 2H), 1.73–1.54 (m, 2H), 0.93–0.81 (m, 2H), 0.72–0.62 (m, 2H). HRMS (ESI-FTMS) *m/z* [M + H]⁺ Calcd for C₃₀H₃₄O₄N₂FS 537.2218; Found 537.2217.

4-((1-Benzylazetid-3-yl)methoxy)-5-cyclopropyl-2-fluoro-N-(methylsulfonyl)benzamide (11). Compound 11 was prepared using the general procedure for the synthesis of 9, substituting S1 for (1-benzylazetid-3-yl)methanol in the reaction preparing S2 (see Supporting Information). ¹H NMR (400 MHz, DMSO-*d*₆) δ 7.49–7.31 (m, 5H), 7.23 (d, *J* = 8.5 Hz, 1H), 6.80 (d, *J* = 12.7 Hz, 1H), 4.18 (d, *J* = 6.1 Hz, 2H), 4.08 (s, 2H), 3.92–3.78 (m, 2H), 3.68 (d, *J* = 8.1 Hz, 2H), 3.18–3.05 (m, 1H), 2.99 (s, 3H), 2.11–1.94 (m, 1H), 0.94–0.81 (m, 2H), 0.65–0.53 (m, 2H). Exchangeable NH not observed. HRMS (ESI-FTMS) *m/z* [M + H]⁺ Calcd for C₂₂H₂₆O₄N₂FS 433.1592; Found 433.1583.

4-((1-Benzylpiperidin-4-yl)methoxy)-5-cyclopropyl-2-fluoro-N-(methylsulfonyl)benzamide (12). Compound 12 was prepared using the general procedure for the synthesis of 2, substituting 31 for benzyl chloride in the reaction preparing 32. ¹H NMR (300 MHz, CDCl₃) δ 7.55 (d, *J* = 9.04 Hz, 1H), 7.44–7.36 (m, 5H), 6.52 (d, *J* = 14.25 Hz, 1H), 4.16–4.02 (m, 2H), 3.94–3.86 (m, 2H), 3.64–3.43 (m, 2H), 3.39 (s, 3H), 2.68–2.43 (m, 2H), 2.09–1.87 (m, 6H), 0.97–0.85 (m, 2H), 0.65–0.55 (m, 2H). Exchangeable NH not observed. HRMS (ESI-FTMS) *m/z* [M + H]⁺ Calcd for C₂₄H₃₀O₄N₂FS 461.1905; Found 461.1896.

4-((1-(4-Chlorobenzyl)piperidin-4-yl)methoxy)-5-cyclopropyl-2-fluoro-N-(methylsulfonyl)benzamide (13). Compound 13 was prepared using the general procedure for the synthesis of 2, substituting 31 for *p*-chlorobenzyl chloride in the reaction preparing 32. ¹H NMR (400 MHz, DMSO-*d*₆) δ 7.42 (d, *J* = 8.5 Hz, 2H), 7.37 (d, *J* = 8.5 Hz, 2H), 7.19 (d, *J* = 8.5 Hz, 1H), 6.78 (d, *J* = 12.8 Hz, 1H), 3.91 (d, *J* = 5.9 Hz, 2H), 3.67 (s, 2H), 3.08–2.87 (m, 6H), 2.31–2.14 (m, 2H), 2.00 (tt, *J* = 8.5, 5.4 Hz, 1H), 1.89–1.73 (m, 3H), 1.41 (d, *J* = 12.5 Hz, 2H), 0.93–0.81 (m, 2H), 0.65–0.52 (m, 2H). HRMS (ESI-FTMS) *m/z* [M + H]⁺ Calcd for C₂₄H₂₉O₄N₂ClFS 495.1515; Found 495.1513.

5-Cyclopropyl-2-fluoro-N-(methylsulfonyl)-4-((1-(4-(trifluoromethoxy)benzyl)piperidin-4-yl)methoxy)benzamide (14). Compound 14 was prepared using the general procedure for the synthesis of 2, substituting 31 for 1-(chloromethyl)-4-

(trifluoromethoxy)benzene in the reaction preparing **32**. ^1H NMR (400 MHz, DMSO- d_6) δ 10.91 (s, 1H), 7.55–7.46 (m, 2H), 7.38 (d, $J = 8.1$ Hz, 2H), 7.17 (d, $J = 8.4$ Hz, 1H), 6.85 (d, $J = 12.8$ Hz, 1H), 3.94 (d, $J = 6.0$ Hz, 2H), 3.81 (s, 2H), 3.12 (s, 3H), 3.04 (d, $J = 11.5$ Hz, 2H), 2.37 (s, 2H), 2.01 (tt, $J = 8.5, 5.3$ Hz, 1H), 1.94–1.81 (m, 3H), 1.45 (q, $J = 11.9$ Hz, 2H), 0.94–0.81 (m, 2H), 0.69–0.57 (m, 2H). HRMS (ESI-FTMS) m/z $[\text{M} + \text{H}]^+$ Calcd for $\text{C}_{25}\text{H}_{29}\text{O}_5\text{N}_2\text{F}_4\text{S}$ 545.1728; Found 545.1729.

5-Cyclopropyl-4-((1-(3,5-dichlorobenzyl)piperidin-4-yl)methoxy)-2-fluoro-*N*-(methylsulfonyl)benzamide (15). Compound **15** was prepared using the general procedure for the synthesis of **2**, substituting **31** for 1,3-dichloro-5-(chloromethyl)benzene in the reaction preparing **32**. ^1H NMR (400 MHz, DMSO- d_6) δ 11.43 (s, 1H), 7.53 (t, $J = 2.0$ Hz, 1H), 7.40 (d, $J = 2.0$ Hz, 2H), 7.17 (d, $J = 8.4$ Hz, 1H), 6.86 (d, $J = 12.9$ Hz, 1H), 3.94 (d, $J = 5.9$ Hz, 2H), 3.64 (s, 2H), 3.15 (s, 3H), 2.93 (d, $J = 11.2$ Hz, 2H), 2.19 (s, 2H), 2.01 (tt, $J = 8.4, 5.3$ Hz, 1H), 1.81 (d, $J = 12.6$ Hz, 3H), 1.41 (q, $J = 11.8$ Hz, 2H), 0.93–0.79 (m, 2H), 0.70–0.58 (m, 2H). HRMS (ESI-FTMS) m/z $[\text{M} + \text{H}]^+$ Calcd for $\text{C}_{24}\text{H}_{28}\text{O}_4\text{N}_2\text{Cl}_2\text{FS}$ 529.1125; Found 529.1127.

5-Cyclopropyl-4-((1-(3,5-dichlorobenzyl)piperidin-4-yl)methoxy)-2-fluoro-*N*-(methylsulfonyl)benzamide (16). Compound **16** was prepared from **S6** and following the general procedure for the synthesis of **2**, analogous to the sequence beginning with **32**. See [Supporting Information](#) for the synthesis of **S6**. ^1H NMR (400 MHz, DMSO- d_6) δ 11.87 (s, 1H), 7.71 (t, $J = 1.9$ Hz, 1H), 7.45 (d, $J = 1.9$ Hz, 2H), 7.15 (d, $J = 8.3$ Hz, 1H), 6.94 (d, $J = 12.9$ Hz, 1H), 4.48 (d, $J = 12.8$ Hz, 1H), 3.98 (d, $J = 6.3$ Hz, 2H), 3.52 (d, $J = 13.2$ Hz, 1H), 3.28 (s, 3H), 3.12 (s, 1H), 2.84 (s, 1H), 2.15–1.96 (m, 2H), 1.95–1.83 (m, 1H), 1.76 (d, $J = 12.3$ Hz, 1H), 1.35 (s, 2H), 0.94–0.84 (m, 2H), 0.74–0.61 (m, 2H). HRMS (ESI-FTMS) m/z $[\text{M} + \text{H}]^+$ Calcd for $\text{C}_{24}\text{H}_{26}\text{O}_3\text{N}_2\text{Cl}_2\text{FS}$ 543.0918; Found 543.0920.

5-Cyclopropyl-4-((1-(2-(3,5-dichlorophenyl)propan-2-yl)piperidin-4-yl)methoxy)-2-fluoro-*N*-(methylsulfonyl)benzamide (17). Compound **17** was prepared from **S7** and following the general procedure for the synthesis of **2**, analogous to the sequence beginning with **32**. See [Supporting Information](#) for the synthesis of **S7**. ^1H NMR (400 MHz, DMSO- d_6) δ 11.85 (s, 1H), 7.51 (s, 2H), 7.45 (s, 1H), 7.16 (d, $J = 8.4$ Hz, 1H), 6.90 (d, $J = 12.9$ Hz, 1H), 3.94 (d, $J = 5.7$ Hz, 2H), 3.24 (s, 3H), 2.75 (s, 2H), 2.19–2.06 (m, 1H), 2.01 (tt, $J = 8.5, 5.4$ Hz, 1H), 1.82–1.74 (m, 4H), 1.46–1.16 (m, 8H), 0.97–0.79 (m, 2H), 0.74–0.57 (m, 2H). HRMS (ESI-FTMS) m/z $[\text{M} + \text{H}]^+$ Calcd for $\text{C}_{26}\text{H}_{32}\text{O}_4\text{N}_2\text{Cl}_2\text{FS}$ 557.1438; Found 557.1443.

(*R*)-5-Cyclopropyl-4-((1-(1-(3,5-dichlorophenyl)ethyl)piperidin-4-yl)methoxy)-2-fluoro-*N*-(methylsulfonyl)benzamide (18). Compound **18** was prepared using the general procedure for the synthesis of **2**, substituting **31** for its enantiomer—which could be prepared from an identical sequence as **31** using the (*R*)-CBS catalyst—in the reaction preparing **32**. ^1H NMR (400 MHz, DMSO- d_6) δ 7.54 (s, 1H), 7.43 (s, 2H), 7.15 (d, $J = 8.4$ Hz, 1H), 6.87 (d, $J = 12.9$ Hz, 1H), 3.92 (d, $J = 5.8$ Hz, 2H), 3.78 (s, 1H), 3.20 (s, 3H), 3.11–3.06 (m, 1H), 3.00–2.81 (m, 1H), 2.18–2.12 (m, 2H), 2.00 (tt, $J = 8.5, 5.3$ Hz, 1H), 1.90–1.72 (m, 3H), 1.37 (d, $J = 6.3$ Hz, 5H), 0.92–0.81 (m, 2H), 0.71–0.59 (m, 2H). Exchangable NH not observed. HRMS (ESI-FTMS) m/z $[\text{M} + \text{H}]^+$ Calcd for $\text{C}_{25}\text{H}_{30}\text{O}_4\text{N}_2\text{Cl}_2\text{FS}$ 543.1282; Found 543.1281.

***tert*-Butyl-5-chloro-2,4-difluorobenzoate (20)**. To a stirred solution of 5-chloro-2,4-difluorobenzoic acid (**19**, 200 g, 1.04 mol) in *t*-BuOH (1 L) was added (Boc) $_2$ O (453 g, 2.08 mol), and then DMAP (26 g, 0.208 mmol) was added slowly to the mixture. The reaction was heated to 60 °C and stirred overnight. The mixture was concentrated to give a crude product; water and EtOAc were added, and the aqueous layer was extracted with EtOAc. The organic layer was combined and dried over anhydrous Na_2SO_4 , filtered, and concentrated under reduced pressure. The residue was purified by column chromatography eluting with petroleum ether/EtOAc = 1:1 to give compound **20** (232 g, 90% yield) as a yellow oil. ^1H NMR (300 MHz, CDCl_3) δ 7.94 (t, $J = 7.8$ Hz, 1H), 6.95 (t, $J = 9.4$ Hz, 1H), 1.59 (s, 9H).

***tert*-Butyl-4-((adamantan-1-yl)methoxy)-5-chloro-2-fluorobenzoate (21)**. To a solution of **20** (230 g, 0.927 mol) in anhydrous dimethyl sulfoxide (1 L) was added 1-adamantane methanol (154 g, 0.927 mol) and Cs_2CO_3 (393g, 1.20 mol), and the suspension was stirred at 80 °C for 4 h. Water and EtOAc were added to the mixture, and the aqueous layer was extracted with EtOAc. The combined organic layers were dried and concentrated to give a crude residue, which was triturated with methanol. The resulting white solid was filtered and dried to give **21** (193 g, 52% yield). ^1H NMR (300 MHz, CDCl_3) δ 7.84 (d, $J = 7.8$ Hz, 1H), 6.59 (d, $J = 12.3$ Hz, 1H), 3.53 (s, 2H), 2.01 (s, 3H), 1.78–1.61 (m, 12H), 1.55 (s, 9H).

***tert*-Butyl-4-((adamantan-1-yl)methoxy)-5-cyclopropyl-2-fluorobenzoate (22)**. To a solution of **21** (15.80 g, 40 mmol), cyclopropylboronic acid (5.16 g, 60 mmol), potassium phosphate (38.2 g, 180 mmol) and tricyclohexylphosphine tetrafluoroborate (1.47 g, 3.99 mmol) in toluene (160 mL) and water (8 mL) under a nitrogen atmosphere was added palladium acetate (0.45 g, 2.00 mmol). The reaction mixture was heated to 100 °C for 18 h and then cooled to ambient temperature. Water was added, and the mixture extracted with ethyl acetate, the combined organics were washed with brine; dried over anhydrous Na_2SO_4 and concentrated. Purification of the residue by column chromatography (5% ethyl acetate in hexanes) afforded **22** (13.8 g, 86% yield). ^1H NMR (300 MHz, CDCl_3) δ 7.37 (d, $J = 8.4$ Hz, 1H), 6.47 (d, $J = 12.9$ Hz, 1H), 3.49 (s, 2H), 2.05–1.95 (m, 4H), 1.78–1.61 (m, 12H), 1.55 (s, 9H), 0.91–0.84 (m, 2H), 0.64–0.58 (m, 2H).

4-((Adamantan-1-yl)methoxy)-5-cyclopropyl-2-fluorobenzoic acid (23). To a solution of **22** (257g, 642 mmol) in dichloromethane (500 mL), was added trifluoroacetic acid (250 mL). The reaction mixture was stirred at ambient temperature for 2 h and then concentrated in vacuo. The residue was triturated in methanol (500 mL), and the solid was filtered and dried to give **23** (158 g, 71% yield). ^1H NMR (300 MHz, DMSO- d_6) δ 12.77 (s, 1H), 7.29 (d, $J = 8.4$ Hz, 1H), 6.83 (d, $J = 13.2$ Hz, 1H), 3.59 (s, 2H), 2.04–1.92 (m, 4H), 1.71–1.58 (m, 12H), 0.91–0.83 (m, 2H), 0.59–0.52 (m, 2H). LCMS m/z 345.1 $[\text{M} + \text{H}]^+$.

***tert*-Butyl-4-((4-(*tert*-butoxycarbonyl)-2-chloro-5-fluorophenoxy)methyl)piperidine-1-carboxylate (26)**. To a mixture of **20** (10.0 g, 46.3 mmol) and **25** (12.6 g, 50.9 mmol) in DMSO (200 mL) was added Cs_2CO_3 (18.1 g, 55.6 mmol). The reaction mixture was stirred at rt for 1 h, poured into ice-water, and extracted with EtOAc. The combined organics were washed with brine, dried over anhydrous Na_2SO_4 , and concentrated. The crude residue was purified by silica gel chromatography (eluting with petroleum ether/EtOAc, from 20/1 to 5/1) to give **26** (12.3 g, 60%) as yellow oil. ^1H NMR (300 MHz, CDCl_3) δ 7.85 (d, $J = 7.6$ Hz, 1H), 6.59 (d, $J = 11.9$ Hz, 1H), 4.23–4.05 (m, 2H), 3.84 (d, $J = 6.2$ Hz, 2H), 2.81–2.64 (m, 2H), 2.10–1.94 (m, 1H), 1.87–1.77 (m, 2H), 1.55 (s, 9H), 1.44 (s, 9H), 1.36–1.20 (m, 2H). LCMS m/z 466.1 $[\text{M} + \text{Na}]^+$.

***tert*-Butyl-4-((1-benzylpiperidin-4-yl)methoxy)-5-cyclopropyl-2-fluorobenzoate (27)**. To a mixture of **26** (5 g, 11.3 mmol), cyclopropylboronic acid (2.91 g, 33.9 mmol), K_3PO_4 (7.18 g, 339 mmol), and $\text{P}(\text{Cy})_3\text{-HBF}_4$ (1.81g, 4.5 mmol) in toluene (200 mL) and water (10 mL) under N_2 was added $\text{Pd}(\text{OAc})_2$ (230 mg, 1.13 mmol). The reaction mixture was heated to 100 °C for 16 h and cooled to rt. Water was added, and the mixture was extracted with ethyl acetate. The combined organics were washed with brine, dried over anhydrous Na_2SO_4 , and concentrated. The residue was purified by silica gel chromatography (eluting with petroleum ether/EtOAc, from 10/1 to 2/1) to give **27** (3.7 g, 74%) as yellow oil. LCMS m/z 472.2 $[\text{M} + \text{Na}]^+$.

Methyl-5-cyclopropyl-2-fluoro-4-(piperidin-4-ylmethoxy)benzoate (28). To a solution of **27** (9.0 g, 20.0 mmol) in MeOH (110 mL) was added SOCl_2 (10 mL) dropwise. The reaction mixture was stirred at reflux for 16 h, cooled to rt, and concentrated. The residue was slurried in petroleum ether/ethyl acetate (20/1), filtered, and dried to give **28** (4.3 g, 70% yield) as a HCl salt and gray solid. LCMS m/z 308.2 $[\text{M} + \text{H}]^+$.

(R)-1-(3,5-Dichlorophenyl)ethan-1-ol (30). A 1 M solution of (S)-2-methyl-CBS-oxazaborolidine (84.6 mL, 84.6 mmol) in toluene and BH₃-DMS (47.3 mL, 508 mmol) were dissolved in THF (1.4 L). The mixture was stirred at 20 °C for 30 min before the addition of a solution of **29** (80.0 g, 423 mmol) in THF (500 mL) dropwise over 1.5 h. The mixture was stirred at 20 °C for 2 h. The mixture was quenched with MeOH dropwise at 0 °C, followed by the addition of 2 M HCl. The mixture was extracted with DCM, washed with water and brine, dried over anhydrous Na₂SO₄, filtered, and concentrated. The crude product was heated in MeOH followed by the addition of water to precipitate **30** (63.1 g, 79% yield) as a white solid. ¹H NMR (400 MHz, CDCl₃) δ 7.26 (s, 3H), 4.85 (q, *J* = 6.4 Hz, 1H), 2.19–1.97 (m, 1H), 1.48 (d, *J* = 6.4 Hz, 3H). SFC analysis showed the product was 98.3% ee.

(R)-1-(3,5-Dichlorophenyl)ethylmethanesulfonate (31). To a solution of **30** (6.7 g, 35 mmol) and Ms₂O (6.7 g, 38.5 mmol) in DCM (175 mL) at 0 °C was added Et₃N (5.4 mL, 38.5 mmol) dropwise. The reaction was allowed to warm to rt and stirred for 2 h. Saturated NH₄Cl solution (20 mL) was added, and the solution was extracted with DCM. The organic layer was collected, dried with MgSO₄, and concentrated to produce **31** as a clear, colorless oil (8.8 g, 94% yield). ¹H NMR (400 MHz, CDCl₃) δ 7.36 (t, *J* = 1.9 Hz, 1H), 7.28 (d, *J* = 1.9 Hz, 2H), 5.66 (q, *J* = 6.6 Hz, 1H), 2.90 (s, 3H), 1.69 (d, *J* = 6.6 Hz, 3H), 1.58–1.45 (m, 1H).

Methyl-(S)-5-cyclopropyl-4-((1-(1-(3,5-dichlorophenyl)ethyl)piperidin-4-yl)methoxy)-2-fluorobenzoate (32). To a solution of **28** (7.7 g, 25 mmol) in 4-methyl-2-pentanone (125 mL) were added **31** (8.8 g, 33 mmol), water (12.5 mL), and K₂CO₃ (5.2 g, 37.5 mmol). The mixture was heated to 85 °C and stirred for 16 h. Reaction was diluted with water and extracted with EtOAc. The organic layer was collected, dried with MgSO₄, and concentrated. The crude product was purified by column chromatography to produce **32** as a clear colorless oil (11.8 g, 99% yield). ¹H NMR (400 MHz, CDCl₃) δ 7.44 (d, *J* = 8.4 Hz, 1H), 7.31–7.19 (m, 3H), 6.53 (d, *J* = 12.7 Hz, 1H), 3.90–3.80 (m, 5H), 3.40 (q, *J* = 6.7 Hz, 1H), 3.03 (d, *J* = 11.0 Hz, 1H), 2.82 (d, *J* = 11.3 Hz, 1H), 2.09–1.92 (m, 3H), 1.91–1.75 (m, 4H), 1.51–1.24 (m, 4H), 0.95–0.84 (m, 2H), 0.68–0.59 (m, 2H). LCMS *m/z* 480.2 [M + H]⁺.

(S)-5-Cyclopropyl-4-((1-(1-(3,5-dichlorophenyl)ethyl)piperidin-4-yl)methoxy)-2-fluorobenzoic acid (33). To a solution of **32** (11.8 g, 25 mmol) in THF (100 mL) and water (50 mL) was added NaOH (15 g, 375 mmol). The reaction was then heated to reflux (70 °C) and stirred for 16 h. The crude mixture was allowed to cool to 0 °C, and conc HCl was added to precipitate **33** (11.3 g, 97% yield) as a white solid. ¹H NMR (400 MHz, DMSO-*d*₆) δ 7.45 (dt, *J* = 10.9, 2.0 Hz, 1H), 7.37 (dd, *J* = 7.2, 1.9 Hz, 2H), 7.22 (d, *J* = 8.6 Hz, 1H), 6.73 (d, *J* = 12.5 Hz, 1H), 3.87 (d, *J* = 5.8 Hz, 2H), 3.55 (q, *J* = 6.7 Hz, 1H), 2.93 (d, *J* = 11.1 Hz, 1H), 2.78 (d, *J* = 11.2 Hz, 1H), 2.04–1.85 (m, 3H), 1.83–1.66 (m, 3H), 1.42–1.22 (m, 6H), 0.90–0.81 (m, 2H), 0.59–0.50 (m, 2H). LCMS *m/z* 466.1 [M + H]⁺.

Nav1.X Cell Lines. HEK cell lines stably expressing full-length cDNAs coding each Na_v α subunit were generated as previously described,¹³ except in the cases of hNa_v1.1 and hNa_v1.6, which were purchased as Chinese Hamster Ovary (CHO) cell lines from Chantest (now part of Charles River Laboratories) and Genionics AG, respectively. GenBank accession numbers for α-subunits were: hNa_v1.2 (NM_021007), hNa_v1.4 (NM_000334), hNa_v1.5 (AC137587; SCNSA), and hNa_v1.7 (NM_002977).

Radioligand Binding Assays. Radioligand binding assays were conducted as previously described.^{12,13,16}

Sodium Influx Assays. TREX HEK 293 cells were stably transfected with an inducible expression vector containing the full-length cDNA coding for the desired human sodium channel α-subunit, full-length cDNA coding for inward rectifying potassium channel, Kir1.1, and with an expression vector containing full length cDNA coding for the β₁-subunit. Sodium channel expressing cell lines were induced with tetracycline (1 μg/mL) and plated on 384-well poly-D-lysine (PDL)-coated plates at a density of 25K cells/well in culture media (DMEM, containing 10% FBS and 1% L-glutamine).

After overnight incubation (37°C, 5% CO₂), culture media was removed and cells were loaded with 5 μM ANG2 dye for 1 h in Buffer 1 (155 mM NMDG (*N*-methyl-D-glucamine), 5 mM KCl, 2 mM CaCl₂, 1 mM MgCl₂, 10 mM HEPES (4-(2-hydroxyethyl)-1-piperazineethanesulfonic acid buffer), 10 mM glucose, adjusted with Tris to pH 7.4). Excess dye was removed, and cells were incubated with and without test compound for 1 h in Buffer 1 containing 50 μM veratridine or 500 nM veratridine plus 100 nM anthropleurin C for hNa_v1.7 and hNa_v1.5 cells, respectively, at room temperature. A Hamamatsu FDSS μCell was used to perform a 1:1 addition of Na/K challenge buffer (145 mM NaCl, 20 mM HEPES, 1 mM CaCl₂, 15 mM KCl, 1 mM MgCl₂, 10 mM glucose, adjusted with Tris to pH 7.4) and simultaneously read plates at excitation wavelength of 530 nm and emission wavelength of 558 nm. Nonsodium channel mediated sodium influx was determined in the presence of 1 μM tetrodotoxin (TTX) for Na_v1.7 and 25 μM TTX for Na_v1.5. This background signal was subtracted from the total sodium influx signal in the absence of compound, and all data in the presence of compound was normalized to this control. Percent inhibition of sodium ion influx was calculated for each test compound at each test concentration to determine the IC₅₀ values. The use of veratridine and anthropleurin C in the influx assay but not in the voltage clamp studies and the longer time course of the influx assay presumably account for the difference in selectivity between Na_v1.7 and Na_v1.5 in the two assays. For Protein Shift (FluxPS) experiments, 3 mg/mL human serum albumin was added to Buffer 1.

The percent inhibition in the sodium influx assays was determined and IC₅₀ values were calculated using a 4-parameter logistic model using IDBS XLfit integrated with Microsoft Excel 2013: % inhibition = (A + ((B - A)/(1 + (x/C)^D))), where A and B are the maximum and minimum inhibition, respectively; C is the IC₅₀ concentration; D is the (Hill) slope; and x is the concentration of test compound.

Voltage Clamp Whole Cell Recordings. Cell Lines. Electrophysiology experiments were performed with human embryonic kidney cells (HEK), permanently transfected with an expression vector containing the full-length cDNA coding for the human sodium channel α-subunit, grown in culture media containing 10% FBS, 1% PSG, and 0.5 mg/mL G418 at 37 °C with 5% CO₂. The β₁ subunit was coexpressed in all cell lines. The hNa_v1.6 cell line (NM_014191) was purchased as a CHO cell line from Genionics.

Whole Cell Recordings. Sodium currents were measured using the patch clamp technique in the whole-cell configuration using the PatchXpress (PX) automated voltage clamp amplifier. The pipet was filled with a solution comprised of: 5 mM NaCl, 10 mM CsCl, 120 mM CsF, 0.1 mM CaCl₂, 2 mM MgCl₂, 10 mM HEPES, 10 mM EGTA; and adjusted to pH 7.2 with CsOH. The external solution had the following composition: 140 mM NaCl, 5 mM KCl, 2 mM CaCl₂, 1 mM MgCl₂, 10 mM HEPES; and adjusted to pH 7.4 with NaOH. Generally, in studies by PX, the external sodium was reduced by equimolar replacement with choline. Osmolarity in the internal and external solutions was adjusted to 300 and 310 mOsm/kg with glucose, respectively.

Currents were recorded at 40 kHz sampling frequency, filtered at 5 Hz, and stored using a Digidata-1322A analogue/digital interface with the pClamp software (Axon Instruments). Series resistance compensation was applied at 55%. For inactivated state block, general holding voltages were -60 mV (Na_v1.7 and Na_v1.5), -35 mV (Na_v1.1, Na_v1.2, and Na_v1.6), and -50 mV (Na_v1.4). Test pulses were preceded by a 20 ms hyperpolarization to -150 mV to remove fast inactivation.

Data Analysis. For voltage clamp studies, percent inhibition was determined at the holding potential for near complete inactivation and fast inactivation of compound-free channels was removed by a brief, strong hyperpolarization. When analyzing grouped data, IC₅₀ values were determined at different concentrations for multiple cells and a single dose-response curve was generated in Prism software using equation ($I/I_0 = 1/(1 + 10^{((\text{LogIC}_{50} - X) \times \text{Hill slope}))}$); I/I_0 is the fraction of sodium current remaining in the presence of drug, [Drug] is the concentration of drug, LogIC₅₀ is the log of the IC₅₀ concentration, and *n* is the Hill coefficient describing the

stoichiometry of compound binding to the sodium channel. IC_{50} values on the PatchXpress automated voltage-clamp platform were generated from Hill equation fits to pooled data, for which SD is not applicable.

LogD and pK_a . LogD measurements were determined as previously described.²³ pK_a values were determined using published UV-metric procedures.²⁴

Metabolic Stability Study in Liver Microsomes. In vitro metabolism was evaluated in pooled liver microsomes (Celsis, Chicago, IL) from humans ($n = 150$; BioIVT, Hicksville, NY). The incubation mixture was prepared in 0.1 M-potassium phosphate buffer (pH 7.4) containing 0.5 mg/mL microsomal protein, 1 mM NADPH, and 1 μ M of compound. Reactions were initiated with the addition of NADPH. Samples were incubated at 37 °C and aliquots were sampled at 0, 20, 40, and 60 min. Reactions were quenched with 95/5 acetonitrile/water (v/v) containing propranolol as the internal standard at each time point. Samples were centrifuged at 3000g for 10 min. Supernatant was diluted with water (1:2 ratio) and the percentage of G# remaining was determined by LC-MS/MS using the $t = 0$ peak area ratio values as 100%. The in vitro Cl_{int} and scaled hepatic Cl were determined as previously described;^{25,26} standard deviation is not applicable.

Metabolic Stability Study in Cryopreserved Hepatocytes. Metabolic stability was evaluated in cryopreserved hepatocytes from Sprague-Dawley rats, cynomolgus monkey, Beagle dog (Invitrogen Corporation, Carlsbad, CA), and humans (Celsis, Baltimore, MD). The cells were seeded at a density of 0.5×10^6 cells/mL; reactions were initiated with the addition of test compound at a final substrate concentration of 1 μ M. Samples were incubated at 37 °C in 5% carbon dioxide with saturating humidity, and aliquots were sampled at 0, 1, 2, and 3 h. Reactions were quenched with acetonitrile containing propranolol as the internal standard at each time point. Samples were centrifuged at 3000g for 10 min. Supernatant was diluted with water (1:2 ratio), and the percentage of test compound remaining was determined by LC/MS/MS. Using the $t = 0$ peak area ratio values as 100%, the in vitro Cl_{int} and scaled hepatic Cl_{hep} were determined as previously described;^{25,26} standard deviation is not applicable.

In Vitro Plasma Protein Binding. Equilibrium dialysis was conducted using a Single-Use Plate Rapid Equilibrium Dialysis (RED) device (Thermo Scientific, Rockford, IL). In brief, 300 μ L of plasma (set at pH 7.4) spiked with drug (final concentration of 5 μ M) was in the donor chamber, and 500 μ L phosphate buffered saline containing 133 mM potassium phosphate and 150 mM NaCl was in the receiver chamber. The RED device was placed on a shaking incubator at 37 °C with 5% CO₂ at 450 rpm (VWR SymphonyTM). Following 6-h incubation, plasma and buffer samples from the RED device were equalized with equal amount of either blank buffer and plasma, respectively. Samples were then quenched in 1:3 (sample: acetonitrile) ratio with ice cold HPLC grade acetonitrile (EMD Millipore, Billerica, MA) with propranolol as the internal standard. The resulting mixture was shaken for 15 min at 500 rpm (Thermo Scientific Compact Digital MicroPlate Shaker), and the supernatant was collected by centrifuging for 15 min at 3750 rpm (Beckman Coulter Allegra X 12R). Subsequently, the supernatant was diluted with water (1:2 ratio), for LC-MS/MS analysis. Fraction unbound was calculated by dividing the peak area from the receiver chamber by the peak area from the donor chamber. Experiments were conducted in triplicate.

Use of Animal Subjects. All studies involving animals were either approved by the Animal Care Committee of Xenon Pharmaceuticals (Burnaby, BC, Canada) and performed in compliance with the Canadian Council on Animal Care guidelines or approved by the Institutional Animal Care and Use Committee of Genentech (South San Francisco, CA, United States) and performed in accordance with the recommendations of the International Association for the Study of Pain.

Pharmacokinetic Studies in Mouse, Rat, Dog, and Cyno.
Mouse PK. Male FVB mice between 6 and 7 weeks of age with body weight ranging from 23 to 30 g were obtained from Charles River Laboratories (Hollister, CA). Animals were divided into groups of 3

per route and dose, and were not fasted before dosing. Mice were administered compounds intravenously (IV) at 1 mg/kg (formulated in 5% DMSO, 35% PEG400, and 60% phosphate buffered saline) or post oral (PO) at 5 mg/kg (formulated in 0.5% (w/v) methylcellulose, 0.2% (w/v) Tween 80 in water (MCT)) at a dose volume of 5 mL/kg. Blood samples (15 μ L) were collected via tail nick from each animal at 0.25, 0.5, 1, 2, 4, and 6 h postdose and added to 60 μ L of EDTA (1.7 mg/mL) water. Test article concentration in each blood sample was determined by a nonvalidated LCMS/MS assay at Genentech.

Rat PK. Male Sprague-Dawley (SD) rats (9–11 weeks old) ranging from 250 to 300 g were obtained from Charles River Laboratories (Hollister, CA). Animals were fasted overnight before oral dose administration of compounds. Three rats were administered compounds intravenously (IV) at 1 mg/kg (formulated in 10% DMSO, 50% PEG400, and 40% phosphate buffered saline) or post oral (PO) at 5 mg/kg (formulated in MCT). Blood samples (approximately 0.2 mL per sample) were collected from each animal into tubes containing K₂EDTA at 0.033, 0.083, 0.25, 0.5, 1, 2, 4, 6, and 8 h after dose administration. Blood was centrifuged for 10 min to harvest plasma. The concentration of test compound in each plasma sample was determined by a nonvalidated LCMS/MS assay at Genentech. Pharmacokinetic analysis was performed at Genentech using noncompartmental methods.

Dog PK. Pharmacokinetics of test compound was determined in male Beagle dogs following a single IV (formulated in 10% DMSO, 50% PEG400, and 40% PBS) or oral (formulated in 0.5% (w/v) methylcellulose, 1.0% (w/v) Tween 80 in Water) administration. Non-naive male Beagle dogs ages ranging from 6 months to 3 years old and weighing between 6 and 12 kg were obtained from Marshall Bioresources (Beijing, China). Animals were not fasted before IV dosing. They were fasted overnight prior to PO dosing through approximately 4 h postdose.

Blood samples were collected in tubes containing K₂EDTA at predose and at 0.033 (IV only), 0.083, 0.25, 0.5, 1, 3, 6, 9, and 24 h post IV or oral administration. Blood was centrifuged for 10 min to harvest plasma. The concentration of test compound in each plasma sample was determined by a nonvalidated LCMS/MS assay at Wuxi AppTech, Inc. Pharmacokinetic analysis was performed at Genentech using noncompartmental methods.

Cyno PK. Pharmacokinetics of test compound was determined in male cynomolgus monkey following a single 0.5 mg/kg IV (formulated in 10% DMSO, 50% PEG400 and 40% PBS) or 0.5 mg/kg oral (formulated in 0.5% (w/v) methylcellulose, 1.0% (w/v) Tween 80 in water) administration. Non-naive male cynomolgus monkeys ages greater than 2 years old and weighing between 2.5 and 6 kg were obtained from Hainan Jingang Laboratory Animal Co. Ltd. (Hainan, China). Animals were not fasted before IV dosing, but were fasted overnight prior to PO dosing through approximately 4 h postdose. Blood samples were collected in tubes containing K₂EDTA at predose and at 0.033 (IV only), 0.083, 0.25, 0.5, 1, 3, 6, 9, and 24 h post IV or oral administration. Blood was centrifuged for 10 min to harvest plasma. The concentration of test compound in each plasma sample was determined by a nonvalidated LCMS/MS assay at Wuxi AppTech, Inc. Pharmacokinetic analysis was performed at Genentech using noncompartmental methods.

PK/PD Studies in Human Nav1.7 I848T (IEM) Transgenic Mice. Transgenic mice were prepared as described previously.²⁰ Male and female FVB *hSCN9a* transgenic mice used for the experiments were seven to 10 weeks old and weighed 20–30 g. The test compound was administered post oral (PO) in 0.5% w/w methyl cellulose and 0.2% v/v Tween 80 in deionized water (MCT) at a dose volume of 10 mL/kg. An injection of 20 μ L of 39 μ M aconitine (Sigma-Aldrich) was made subcutaneously into the dorsum of the hind paw at the predicted T_{max} after oral test compound administration (as determined previously in separate PK experiments). Video data acquisition begins immediately after injection of aconitine and continues for up to 70 min. The first 30 min of each video (or the 5 min period spanning 10–15 min after aconitine injection) was analyzed and scored for the number of instances of

flicking or lifting the injected paw, or paw licking that lasts for 3 s. At the end of the observation period, mice were euthanized by CO₂ inhalation. Blood samples were collected via cardiac puncture into K₂EDTA tubes and processed into plasma by centrifugation at 17 000g for 2 min and collection of supernatant. Plasma samples were stored at –80 °C until bioanalysis by LC MS/MS to determine test compound concentration.

■ ASSOCIATED CONTENT

SI Supporting Information

The Supporting Information is available free of charge at <https://pubs.acs.org/doi/10.1021/acs.jmedchem.1c00049>.

Additional synthetic methods, plasma exposure of in vivo PK/PD studies, X-ray structure determination of **2**, HPLC purity of tested compounds, representative HPLC chromatograms, NMR spectra of **1** and **2**, and modeling of compounds in the active site of CYP2C8 (PDF)

SMILES molecular formula strings (CSV)

■ AUTHOR INFORMATION

Corresponding Authors

Steven J. McKerrall – Genentech, Inc., South San Francisco, California 94080, United States; orcid.org/0000-0002-2966-5810; Phone: (650) 467-4347;

Email: mckerrall.steven@gene.com

Daniel P. Sutherlin – Genentech, Inc., South San Francisco, California 94080, United States; Phone: (650) 225-3171; Email: sutherlin.dan@gene.com

Authors

Brian S. Safina – Genentech, Inc., South San Francisco, California 94080, United States

Shaoyi Sun – Xenon Pharmaceuticals, Inc., Burnaby, British Columbia V5G 4W8, Canada

Chien-An Chen – Chempartner, Shanghai 201203, P.R. China

Sultan Chowdhury – Xenon Pharmaceuticals, Inc., Burnaby, British Columbia V5G 4W8, Canada

Qi Jia – Xenon Pharmaceuticals, Inc., Burnaby, British Columbia V5G 4W8, Canada

Jun Li – Genentech, Inc., South San Francisco, California 94080, United States

Alla Y. Zenova – Xenon Pharmaceuticals, Inc., Burnaby, British Columbia V5G 4W8, Canada

Jean-Christophe Andrez – Xenon Pharmaceuticals, Inc., Burnaby, British Columbia V5G 4W8, Canada

Girish Bankar – Xenon Pharmaceuticals, Inc., Burnaby, British Columbia V5G 4W8, Canada

Philippe Bergeron – Genentech, Inc., South San Francisco, California 94080, United States

Jae H. Chang – Genentech, Inc., South San Francisco, California 94080, United States; orcid.org/0000-0003-3457-7695

Elaine Chang – Xenon Pharmaceuticals, Inc., Burnaby, British Columbia V5G 4W8, Canada

Jun Chen – Genentech, Inc., South San Francisco, California 94080, United States

Richard Dean – Xenon Pharmaceuticals, Inc., Burnaby, British Columbia V5G 4W8, Canada

Shannon M. Decker – Xenon Pharmaceuticals, Inc., Burnaby, British Columbia V5G 4W8, Canada

Antonio DiPasquale – Genentech, Inc., South San Francisco, California 94080, United States

Thilo Focken – Xenon Pharmaceuticals, Inc., Burnaby, British Columbia V5G 4W8, Canada; orcid.org/0000-0003-1993-2476

Ivan Hemeon – Xenon Pharmaceuticals, Inc., Burnaby, British Columbia V5G 4W8, Canada

Kuldip Khakh – Xenon Pharmaceuticals, Inc., Burnaby, British Columbia V5G 4W8, Canada

Amy Kim – Genentech, Inc., South San Francisco, California 94080, United States

Rainbow Kwan – Xenon Pharmaceuticals, Inc., Burnaby, British Columbia V5G 4W8, Canada

Andrea Lindgren – Xenon Pharmaceuticals, Inc., Burnaby, British Columbia V5G 4W8, Canada

Sophia Lin – Xenon Pharmaceuticals, Inc., Burnaby, British Columbia V5G 4W8, Canada

Jonathan Maher – Genentech, Inc., South San Francisco, California 94080, United States

Janette Mezeyova – Xenon Pharmaceuticals, Inc., Burnaby, British Columbia V5G 4W8, Canada

Dinah Misner – Genentech, Inc., South San Francisco, California 94080, United States

Karen Nelkenbrecher – Xenon Pharmaceuticals, Inc., Burnaby, British Columbia V5G 4W8, Canada

Jodie Pang – Genentech, Inc., South San Francisco, California 94080, United States

Rebecca Reese – Genentech, Inc., South San Francisco, California 94080, United States

Shannon D. Shields – Genentech, Inc., South San Francisco, California 94080, United States

Luis Sojo – Xenon Pharmaceuticals, Inc., Burnaby, British Columbia V5G 4W8, Canada

Tao Sheng – Xenon Pharmaceuticals, Inc., Burnaby, British Columbia V5G 4W8, Canada

Henry Verschoof – Xenon Pharmaceuticals, Inc., Burnaby, British Columbia V5G 4W8, Canada

Matthew Waldbrook – Xenon Pharmaceuticals, Inc., Burnaby, British Columbia V5G 4W8, Canada

Michael S. Wilson – Xenon Pharmaceuticals, Inc., Burnaby, British Columbia V5G 4W8, Canada

Zhiwei Xie – Xenon Pharmaceuticals, Inc., Burnaby, British Columbia V5G 4W8, Canada

Clint Young – Xenon Pharmaceuticals, Inc., Burnaby, British Columbia V5G 4W8, Canada

Tanja S. Zabka – Genentech, Inc., South San Francisco, California 94080, United States

David H. Hackos – Genentech, Inc., South San Francisco, California 94080, United States

Daniel F. Ortwine – Genentech, Inc., South San Francisco, California 94080, United States

Andrew D. White – Chempartner, Shanghai 201203, P.R. China; orcid.org/0000-0001-7869-0118

J.P. Johnson, Jr. – Xenon Pharmaceuticals, Inc., Burnaby, British Columbia V5G 4W8, Canada

C. Lee Robinette – Xenon Pharmaceuticals, Inc., Burnaby, British Columbia V5G 4W8, Canada

Christoph M. Dehnhardt – Xenon Pharmaceuticals, Inc., Burnaby, British Columbia V5G 4W8, Canada;

orcid.org/0000-0001-5213-6354

Charles J. Cohen – Xenon Pharmaceuticals, Inc., Burnaby, British Columbia V5G 4W8, Canada

Complete contact information is available at:
<https://pubs.acs.org/10.1021/acs.jmedchem.1c00049>

Funding

Thanks to Genentech, a member of the Roche Group, for research funding.

Notes

The authors declare the following competing financial interest(s): The authors are employees of Xenon Pharmaceuticals or Genentech, part of the Roche Group, and may hold stock in those companies.

ACKNOWLEDGMENTS

We would like to thank the members of the synthetic chemistry teams at Shanghai ChemPartner and Xenon Pharmaceuticals. We thank Genentech Analytical, Purification, DMPK, Safety Assessment, and in vivo Studies Group colleagues for their contributions.

ABBREVIATIONS

CIP, congenital insensitivity to pain; EP, electrophysiology; IEM, inherited erythromelalgia; LLE, lipophilic ligand efficiency; PK, pharmacokinetic; PPB, plasma protein binding; RLB, radioligand binding; VSD4, Na_v1.7 fourth voltage sensing domain

REFERENCES

- (1) Dahlhamer, J.; Lucas, J.; Zelaya, C.; Nahin, R.; Mackey, S.; Debar, L.; Kerns, R.; Von Korff, M.; Porter, L.; Helmick, C. Prevalence of chronic Pain and high-impact chronic pain among adults — United States, 2016. *MMWR Morb Mortal Wkly Rep* **2018**, *67*, 1001–1006.
- (2) Wood, J. N.; Boorman, J. P.; Okuse, K.; Baker, M. D. Voltage-gated sodium channels and pain pathways. *J. Neurobiol.* **2004**, *61*, 55–71.
- (3) Cox, J. J.; Reimann, F.; Nicholas, A. K.; Thornton, G.; Roberts, E.; Springell, K.; Karbani, G.; Jafri, H.; Mannan, J.; Raashid, Y.; Al-Gazali, L.; Hamamy, H.; Valente, E. M.; Gorman, S.; Williams, R.; McHale, D. P.; Wood, J. N.; Gribble, F. M.; Woods, C. G. An SCN9A channelopathy causes congenital inability to experience pain. *Nature* **2006**, *444*, 894–898.
- (4) Goldberg, Y. P.; MacFarlane, J.; MacDonald, M. L.; Thompson, J.; Dube, M. P.; Mattice, M.; Fraser, R.; Young, C.; Hossain, S.; Pape, T.; Payne, B.; Radomski, C.; Donaldson, G.; Ives, E.; Cox, J.; Younghusband, H. B.; Green, R.; Duff, A.; Boltshauser, E.; Grinspan, G. A.; Dimon, J. H.; Sibley, B. G.; Andria, G.; Toscano, E.; Kerdraon, J.; Bowsher, D.; Pimstone, S. N.; Samuels, M. E.; Sherrington, R.; Hayden, M. R. Loss-of-function mutations in the Nav1.7 gene underlie congenital indifference to pain in multiple human populations. *Clin. Genet.* **2007**, *71*, 311–319.
- (5) Gingras, J.; Smith, S.; Matson, D. J.; Johnson, D.; Nye, K.; Couture, L.; Feric, E.; Yin, R.; Moyer, B. D.; Peterson, M. L.; Rottman, J. B.; Beiler, R. J.; Malmberg, A. B.; McDonough, S. I. Global Nav1.7 knockout mice recapitulate the phenotype of human congenital indifference to pain. *PLoS One* **2014**, *9*, No. e105895.
- (6) Shields, S. D.; Deng, L.; Reese, R. M.; Dourado, M.; Tao, J.; Foreman, O.; Chang, J. H.; Hackos, D. H. Insensitivity to pain upon adult-onset deletion of Na_v1.7 or its blockade with selective inhibitors. *J. Neurosci.* **2018**, *38*, 10180–10201.
- (7) Bagal, S. K.; Chapman, M. L.; Marron, B. E.; Prime, R.; Storer, R. I.; Swain, N. A. Recent progress in sodium channel modulators for pain. *Bioorg. Med. Chem. Lett.* **2014**, *24*, 3690–3699.
- (8) McKerrall, S. J.; Sutherlin, D. P. Na_v1.7 inhibitors for the treatment of chronic pain. *Bioorg. Med. Chem. Lett.* **2018**, *28*, 3141–3149.

- (9) Swain, N. A.; Batchelor, D.; Beaudoin, S.; Bechle, B. M.; Bradley, P. A.; Brown, A. D.; Brown, B.; Butcher, K. J.; Butt, R. P.; Chapman, M. L.; Denton, S.; Ellis, D.; Galan, S. R. G.; Gaulier, S. M.; Greener, B. S.; de Groot, M. J.; Glossop, M. S.; Gurrell, I. K.; Hannam, J.; Johnson, M. S.; Lin, Z.; Markworth, C. J.; Marron, B. E.; Millan, D. S.; Nakagawa, S.; Pike, A.; Printzenhoff, D.; Rawson, D. J.; Ransley, S. J.; Reister, S. M.; Sasaki, K.; Storer, R. I.; Stuppel, P. A.; West, C. W. Discovery of clinical candidate 4-[2-(5-Amino-1H-pyrazol-4-yl)-4-chlorophenoxy]-5-chloro-2-fluoro-N-1,3-thiazol-4-ylbenzenesulfonamide (PF-05089771): design and optimization of diaryl ether aryl sulfonamides as selective inhibitors of NaV1.7. *J. Med. Chem.* **2017**, *60*, 7029–7042.
- (10) Weiss, M. M.; Dineen, T. A.; Marx, I. E.; Altmann, S.; Boezio, A.; Bregman, H.; Chu-Moyer, M.; DiMauro, E. F.; Feric Bojic, E.; Foti, R. S.; Gao, H.; Graceffa, R.; Gunaydin, H.; Guzman-Perez, A.; Huang, H.; Huang, L.; Jarosh, M.; Kornecook, T.; Kreiman, C. R.; Ligutti, J.; La, D. S.; Lin, M.-H. J.; Liu, D.; Moyer, B. D.; Nguyen, H. N.; Peterson, E. A.; Rose, P. E.; Taborn, K.; Youngblood, B. D.; Yu, V.; Fremeau, R. T. Sulfonamides as selective NaV1.7 inhibitors: optimizing potency and pharmacokinetics while mitigating metabolic liabilities. *J. Med. Chem.* **2017**, *60*, 5969–5989.
- (11) La, D. S.; Peterson, E. A.; Bode, C.; Boezio, A. A.; Bregman, H.; Chu-Moyer, M. Y.; Coats, J.; DiMauro, E. F.; Dineen, T. A.; Du, B.; Gao, H.; Graceffa, R.; Gunaydin, H.; Guzman-Perez, A.; Fremeau, R., Jr.; Huang, X.; Ilch, C.; Kornecook, T. J.; Kreiman, C.; Ligutti, J.; Jasmine Lin, M. H.; McDermott, J. S.; Marx, I.; Matson, D. J.; McDonough, S. I.; Moyer, B. D.; Nguyen, H. N.; Taborn, K.; Yu, V.; Weiss, M. M. The discovery of benzoxazine sulfonamide inhibitors of NaV1.7: tools that bridge efficacy and target engagement. *Bioorg. Med. Chem. Lett.* **2017**, *27*, 3477–3485.
- (12) McKerrall, S. J.; Nguyen, T.; Lai, K. W.; Bergeron, P.; Deng, L.; DiPasquale, A.; Chang, J. H.; Chen, J.; Chernov-Rogan, T.; Hackos, D. H.; Maher, J.; Ortwine, D. F.; Pang, J.; Payandeh, J.; Proctor, W. R.; Shields, S. D.; Vogt, J.; Ji, P.; Liu, W.; Ballini, E.; Schumann, L.; Tarozzo, G.; Bankar, G.; Chowdhury, S.; Hasan, A.; Johnson, J. P.; Khakh, K.; Lin, S.; Cohen, C. J.; Dehnhardt, C. M.; Safina, B. S.; Sutherlin, D. P. Structure- and ligand-based discovery of chromane arylsulfonamide Na_v1.7 inhibitors for the treatment of chronic pain. *J. Med. Chem.* **2019**, *62*, 4091–4109.
- (13) Ahuja, S.; Mukund, S.; Deng, L.; Khakh, K.; Chang, E.; Ho, H.; Shriver, S.; Young, C.; Lin, S.; Johnson, J. P.; Wu, P.; Li, J.; Coons, M.; Tam, C.; Brillantes, B.; Sampang, H.; Mortara, K.; Bowman, K. K.; Clark, K. R.; Estevez, A.; Xie, Z.; Verschoof, H.; Grimwood, M.; Dehnhardt, C.; Andrez, J.-C.; Focken, T.; Sutherlin, D. P.; Safina, B. S.; Starovasnik, M. A.; Ortwine, D. F.; Franke, Y.; Cohen, C. J.; Hackos, D. H.; Koth, C. M.; Payandeh, J. Structural basis of Nav1.7 inhibition by an isoform-selective small-molecule antagonist. *Science* **2015**, *350*, No. aac5464.
- (14) Catterall, W. A.; Dib-Hajj, S.; Meisler, M. H.; Pietrobon, D. Inherited neuronal ion channelopathies: new windows on complex neurological diseases. *J. Neurosci.* **2008**, *28*, 11768–11777.
- (15) Tfelt-Hansen, J.; Winkel, B. G.; Grunnet, M.; Jespersen, T. Inherited cardiac diseases caused by mutations in the Nav1.5 sodium channel. *Journal of Cardiovascular Electrophysiology* **2010**, *21*, 107–115.
- (16) Sun, S.; Jia, Q.; Zenova, A. Y.; Wilson, M. S.; Chowdhury, S.; Focken, T.; Li, J.; Decker, S.; Grimwood, M. E.; Andrez, J. C.; Hemeon, I.; Sheng, T.; Chen, C. A.; White, A.; Hackos, D. H.; Deng, L.; Bankar, G.; Khakh, K.; Chang, E.; Kwan, R.; Lin, S.; Nelkenbrecher, K.; Sellers, B. D.; DiPasquale, A. G.; Chang, J.; Pang, J.; Sojo, L.; Lindgren, A.; Waldbrook, M.; Xie, Z.; Young, C.; Johnson, J. P.; Robinette, C. L.; Cohen, C. J.; Safina, B. S.; Sutherlin, D. P.; Ortwine, D. F.; Dehnhardt, C. M. Identification of selective acyl sulfonamide-cycloalkylether inhibitors of the voltage gated sodium channel (NaV) 1.7 with potent analgesic activity. *J. Med. Chem.* **2019**, *62*, 908–927.
- (17) Melet, A.; Marques-Soares, C.; Schoch, G. A.; Macherey, A.; Jaouen, M.; Dansette, P. M.; Sari, M.; Johnson, E. F.; Mansuy, D. Analysis of human cytochrome P450 2C8 substrate specificity using a

substrate pharmacophore and site-directed mutants. *Biochemistry* **2004**, *43*, 15379–15392.

(18) Bagdanoff, J. T.; Xu, Y.; Dollinger, G.; Martin, E. Effect of chirality on common in vitro experiments: an enantiomeric pair analysis. *J. Med. Chem.* **2015**, *58*, 5781–5788.

(19) Rothenberg, M. E.; Tagen, M.; Chang, J. H.; Boyce-Rustay, J.; Friesenhahn, M.; Hackos, D. H.; Hains, A.; Sutherlin, D.; Ward, M.; Cho, W. Safety, tolerability, and pharmacokinetics of GDC-0276, a novel Nav1.7 inhibitor, in a first-in-human, single- and multiple-dose study in healthy volunteers. *Clin. Drug Invest.* **2019**, *39*, 873–887.

(20) Bankar, G.; Goodchild, S. J.; Howard, S.; Nelkenbrecher, K.; Waldbrook, M.; Dourado, M.; Shuart, N. G.; Lin, S.; Young, C.; Xie, Z.; Khakh, K.; Chang, E.; Sojo, L. E.; Lindgren, A.; Chowdhury, S.; Decker, S.; Grimwood, M.; Andrez, J.; Dehnhardt, C. M.; Pang, J.; Chang, J. H.; Safina, B. S.; Sutherlin, D. P.; Johnson, J. P., Jr.; Hackos, D. H.; Robinette, C. L.; Cohen, C. J. Selective Nav1.7 antagonists with long residence time show improved efficacy against inflammatory and neuropathic pain. *Cell Rep.* **2018**, *24*, 3133–3145.

(21) Stumpf, A.; Cheng, Z. K.; Beaudry, D.; Angelaud, R.; Gosselin, F. Improved synthesis of the Nav1.7 inhibitor GDC-0276 via a highly regioselective SNAr reaction. *Org. Process Res. Dev.* **2019**, *23*, 1829–1840.

(22) Stumpf, A.; St-Jean, F.; Lao, D.; Cheng, Z. K.; Angelaud, R.; Gosselin, F. Practical early development synthesis of Nav1.7 inhibitor GDC-0310. *Synthesis* **2020**, *52*, 3406.

(23) Lin, B.; Pease, J. H. A novel method for high throughput lipophilicity determination by microscale shake flask and liquid chromatography tandem mass spectrometry. *Comb. Chem. High Throughput Screening* **2013**, *16*, 817–825.

(24) Avdeef, A.; Comer, J. E. A.; Thomson, S. J. pH-Metric log P. 3. Glass electrode calibration in methanol-water, applied to pKa determination of water-insoluble substances. *Anal. Chem.* **1993**, *65*, 42–49.

(25) Obach, R. S. Prediction of human clearance of twenty-nine drugs from hepatic microsomal intrinsic clearance data: an examination of in vitro half-life approach and nonspecific binding to microsomes. *Drug Metab. Dispos.* **1999**, *27*, 1350–1359.

(26) Lin, C.; Shi, J.; Moore, A.; Khetani, S. R. Prediction of drug clearance and drug-drug interactions in microscale cultures of human hepatocytes. *Drug Metab. Dispos.* **2016**, *44*, 127–136.